



## ORIGINAL ARTICLE

# Reorganization of Higher-Order Somatosensory Cortex After Sensory Loss from Hand in Squirrel Monkeys

Hui-Xin Qi , Chia-Chi Liao, Jamie L. Reed and Jon H. Kaas

Department of Psychology, Vanderbilt University, Nashville, TN 37240, USA

Address correspondence to Hui-Xin Qi. Email: [huixin.qi@vanderbilt.edu](mailto:huixin.qi@vanderbilt.edu)  [orcid.org/0000-0003-0265-9194](https://orcid.org/0000-0003-0265-9194)

## Abstract

Unilateral dorsal column lesions (DCL) at the cervical spinal cord deprive the hand regions of somatosensory cortex of tactile activation. However, considerable cortical reactivation occurs over weeks to months of recovery. While most studies focused on the reactivation of primary somatosensory area 3b, here, for the first time, we address how the higher-order somatosensory cortex reactivates in the same monkeys after DCL that vary across cases in completeness, post-lesion recovery times, and types of treatments. We recorded neural responses to tactile stimulation in areas 3a, 3b, 1, secondary somatosensory cortex (S2), parietal ventral (PV), and occasionally areas 2/5. Our analysis emphasized comparisons of the responsiveness, somatotopy, and receptive field size between areas 3b, 1, and S2/PV across DCL conditions and recovery times. The results indicate that the extents of the reactivation in higher-order somatosensory areas 1 and S2/PV closely reflect the reactivation in primary somatosensory cortex. Responses in higher-order areas S2 and PV can be stronger than those in area 3b, thus suggesting converging or alternative sources of inputs. The results also provide evidence that both primary and higher-order fields are effectively activated after long recovery times as well as after behavioral and electrocutaneous stimulation interventions.

**Key words:** neuronal responses, plasticity, receptive field, somatotopy, spinal cord injury

## Introduction

Unilateral dorsal column lesions (DCL) at the level of the upper cervical spinal cord that interrupt tactile afferents from one hand initially impair hand use and deactivate cortical responses to tactile stimulation in somatosensory areas 3b and 1. However, hand use and cortical activation recover over weeks to months after lesion (Jain et al. 1997, 2008; Darian-Smith and Brown 2000; Darian-Smith and Ciferri 2005; Qi, Chen et al. 2011; Chen et al. 2012; Qi et al. 2013, 2014). Yet, very little is known about the extents and mechanisms of reactivation in higher-order somatosensory areas such as the secondary somatosensory area (S2) and the parietal ventral (PV) area over long recovery times after such lesions (however, see Tandon et al. 2009). In most mammals studied, including prosimians, primary and secondary somatosensory areas are activated by independent parallel pathways from the thalamus (Garraghty et al. 1991). However, in many higher primates, secondary somatosensory areas have

been reported to depend on activation in primary somatosensory areas (Pons, Garraghty et al. 1987; Burton et al. 1990; Garraghty, Florence, et al. 1990; Garraghty et al. 1991; Pons et al. 1992). In this study, we hypothesized that properties in higher-order somatosensory areas of squirrel monkey strongly reflect the reactivation in primary somatosensory cortex area 3b. To test this hypothesis, we focused on characterizing neuronal responsiveness, receptive field (RF) properties, and somatotopy in the deprived hand regions in areas S2 and PV, and compared these characteristics with those of reactivated primary somatosensory area 3b and higher-order somatosensory area 1 in squirrel monkeys. Additionally, when possible, we made comparisons with neurons in reactivated hand regions of areas 3a and 2/5. Note that we refer to areas 2/5 here due to the difficulties in defining the border anatomically and functionally in the current preparation. An important feature of the present study is that results from area 3b and higher-order areas were

compared within the same subjects, which allowed us to provide a better understanding of the neural mechanisms of the functional recovery and suggest therapeutic treatments for patients after spinal cord injury (SCI).

A basic, but currently unanswered question concerns the parts of the somatosensory system that are involved in the recovery process. There is already clear evidence that many neurons in the cuneate nucleus of the lower brainstem (Xu and Wall 1999; Woods et al. 2000; Darian-Smith and Ciferri 2006; Graziano and Jones 2009; Kambi et al. 2014; Mowery et al. 2014, 2015) and the ventroposterior nucleus of the thalamus are at least partially reactivated (Garraghty and Kaas 1991; Rasmusson 1996a, 1996b; Florence et al. 2000; Jain et al. 2008; see review in Schmid et al. 2016), or largely deactivated due to axonal withdrawal (e.g., Graziano and Jones 2009) after sensory loss. The reactivation depends, in part, on the sprouting and new growth of preserved afferents into the denervated portion of the cuneate nucleus (Jain et al. 2000). The effects of such reactivations at early stations in the ascending somatosensory system could be relayed to area 3b of primary somatosensory cortex and from there to higher-order somatosensory areas. However, this process is unlikely to reflect a simple relay from level to level without modifications. For example, neurons with RFs including more than one body part are less frequently recorded in area 3b than in the ventroposterior nucleus. Thus, the cortical reactivation appears to be more extensive, and exhibits additional reorganization compared with that in the cuneate nucleus and the ventroposterior nucleus, such that a more normal somatotopy occurs in area 3b (Florence et al. 2000). Information from area 3b in anthropoid primates is typically relayed to areas 1 and 2, and then to area 5 (e.g., Pons and Kaas 1986; Padberg et al. 2007) as part of a dorsal stream of processing for guiding motor behavior that involves posterior parietal areas of cortex with projections to premotor and motor areas (Stepniwska et al. 2005, 2016; Gharbawie et al. 2011). Other projections from anterior parietal cortex are to areas in the lateral sulcus, including S2, PV, and ventral somatosensory (VS) areas (Andersen and Buneo 2002; Battaglia-Mayer and Caminiti 2002; Coq et al. 2004). Presumably, the effects of the reactivation and reorganization in area 3b are relayed to higher-order somatosensory areas where further modulations in reactivation patterns are expected, due to combinations of cortical and subcortical inputs and intrinsic connections. While the reactivation of area 1 has been studied in a limited fashion after a median nerve section (Merzenich, Kaas, Wall, Nelson et al. 1983; Merzenich, Kaas, Wall, Sur et al. 1983), the somatotopy of the reactivation differs considerably from that in area 3b. To our knowledge, little is known currently about the reactivations that likely occur in other higher-order somatosensory areas in primates after DCL, except for an important mapping study in macaque monkeys (Tandon et al. 2009), and our collaborative studies on squirrel monkeys (Wang et al. 2013; Yang et al. 2014). Yet, higher-order somatosensory areas undoubtedly have important roles in processing somatosensory stimuli, and in guiding behavior.

Like area 3b, the responsiveness and somatotopy of higher-order cortical areas after sensory loss can be studied with standard single microelectrode mapping methods. In New World owl monkeys and squirrel monkeys, such mapping methods reveal the hand to be represented in considerable detail in areas 3b and 1 (Merzenich et al. 1978, 1987; Kaas et al. 1979). The hand representations in areas 3a, 3b, 1, and 2/5 are all accessible on the cortical surface for mapping. Areas S2 and PV are on the upper bank of the lateral sulcus where they can be studied with deeper electrode penetrations. Each areal

representation has its own characteristic pattern of somatotopic organization (Cusick et al. 1989; Krubitzer and Kaas 1990, 1992; Qi et al. 2002; Coq et al. 2004). The RF sizes and neuron response properties vary across these fields (see Kaas 2004 for review). Here, we used microelectrode mapping methods to determine the reactivation patterns of the hand representations in S2/PV and compare them with those of areas 3b and 1 after sectioning the hand afferents as they travel to the cuneate nucleus in the spinal cord dorsal columns of squirrel monkeys. Lesions at the higher (cranial) level of C4 eliminated most of the inputs from the slowly adapting (SA) and rapidly adapting (RA) cutaneous receptors of the hand. Lesions at lower (caudal) levels of C5–C6 preserved enough afferents from digit 1 and a small portion of digit 2 to maintain cortical activation.

Our findings suggest that the tactile responses in S2/PV primarily depend on the activations in areas 3b and 1 that are from the few surviving primary and secondary spinal cord projections to the cuneate nucleus (e.g., Liao et al. 2015; Liao et al. 2018). The properties of S2/PV neurons differ from those in areas 3b and 1 by having larger RFs, possibly due to convergent inputs from area 3b and 1. Removing areas 3b and 1 deactivates S2/PV (see Kaas 2004 for review). However, S2 and PV also receive considerable inputs from the ventroposterior inferior (VPI) nucleus, which receives nociceptive and tactile inputs from wide dynamic range neurons. Along with other cortical connections, these alternative inputs may modulate the somatotopy and neural response of S2/PV neurons. Areas S2/PV are proposed to be key areas in a networks involved in a memory and object recognition by touch (e.g., Friedman et al. 1986). Thus, treatments that promote the restoration of neural responses in S2/PV could be critical in behavioral recovery and tactile object recognition after DCL.

## Materials and Methods

Subjects were 13 adult male squirrel monkeys (3 *Saimiri sciureus*, 9 *Saimiri boliviensis*, 1 *Saimiri boliviensis puruviensis*). All procedures were approved by the Vanderbilt University Animal Care and Use Committee and followed the guidelines of the National Institutes of Health Guide for the Care and Use of Laboratory Animals. The current study is based on unpublished data collected from areas S2/PV during previous studies of areas 3b and 1. Among these, three monkeys were used for fMRI studies with electrocutaneous stimulation on the digits (Qi et al. 2016); three monkeys were used for behavioral, electrophysiological, and fMRI-BOLD studies with tactile stimulation on the digits (Qi, Chen et al. 2011; Chen et al. 2012; Qi et al. 2013); and six monkeys were used in anatomical studies (Liao et al. 2016, 2018). These previously published data from areas 3b and 1 are only shown for the purpose of comparison. Data from two monkeys (SM-H and SM-G), and all data from S2/PV was never previously reported.

## Intervention Conditions

A reach-to-grasp task was used as a therapeutic rehabilitation for the affected hand (intensive training), or to detect impairments of hand use after sensory loss (non-intensive testing only). Squirrel monkeys use power grip (digits 2–5 and palm) to pick up small objects. Digit 1 usually helps to manipulate or grab larger objects. The training reinforced the use of the entire hand and arm. Three monkeys (SM-J, SM-U, SM-Y; Table 1) underwent intensive training of the impaired hand 5 days per week for 3 months post-lesion, and were tested once a week

Table 1 Subject characteristics

Group	Cases	Recovery time (days)	Lesion extent (est.)	Lesion level	Intervention conditions	Post-lesional impairment		
						1 week	6 weeks	6 months
Intermediate-term Incomplete	SM-A	63	41%	C4	ES	+/-	N/A	N/A
	SM-H (Fig. 2)	142	64%	C5-C6	No	+	-	N/A
	SM-D	56	77%	C5-C6	Tested only	+	-	N/A
	SM-GE	57	79%	C4-C5	ES	+	N/A	N/A
Long-term Incomplete	SM-T (Fig. 3)	321**	61%	rC5	Tested only	+	+	+
	SM-Y	292	65%	C5-C6	Intensive	+	+	-
	SM-U	414	86%	C5	Intensive	+	+	-
Intermediate-term Complete	SM-BB (Fig. 4)	49	98%	rC5	ES	+	NA	N/A
	SM-C	131**	98%	C4	Tested only	+	-	N/A
	SM-O	48	99%	C4	Tested only	+	+	N/A
Long-term complete	SM-RO (Fig. 5)	253	100%	C4	Tested only	+	+	-
	SM-W	266	100%	C4	No	+	+	+
	SM-J	285	100%	C4	Intensive	+	+	+

\*\* two dorsal column lesions were made near the first DCL in monkeys SM-C and SM-T, the interval between two procedures was 44 (SM-T) and 68 days (SM-C), the post-lesion recovery time and behavioral observation were started on the second lesion; ES, electrocutaneous stimulation; "+", deficit observed; "-", no deficit could be detected; "+/-", observed initial deficit that was not sustained for 1 week; N/A, not applicable, no data.

until the final procedure. Another five monkeys (SM-O, SM-C, SM-D, SM-T, SM-RO) underwent non-intensive testing only, consisting of measuring performance 1–2 times per week. See details in Qi et al. 2013. Another three monkeys (SM-A, SM-BB, SM-GE) received low (2 mA) and high (4 mA) electrocutaneous stimulation on the digits before the lesion and three times post-lesion at weeks 2, 4, and 6 for a separate MRI study (see details in Qi et al. 2016). The stimulation was delivered through gold leads and electrode gel (Spectra360, Parker Laboratories, Fairfield NJ) placed on the lateral aspects of a distal finger pad of the affected hand (same side of DCL). Each session had 20 runs, with each run composed of seven alternating 30 s blocks of baseline (stimulation-off) and single digit electrocutaneous stimulation (stimulation-on; 8 Hz train of square wave, 2-ms duration) on digits 1, 2, or 3.

### Dorsal Column Lesion

A unilateral DCL was made under aseptic conditions and general anesthesia (for more details, see Qi, Chen et al. 2011, Liao et al. 2015, 2016). In brief, skin and muscle incisions were made over the back of the neck to expose the dorsal vertebrae of C4–C5. A small opening was made on the dorsal arch of the vertebrae of the spinal cord, and the dura and pia covering the cervical spinal cord were resected. The lesion was made with fine forceps and a pair of surgical iris scissors. The dura was then replaced by Gelfilm, and the incision site was closed. The monkeys were carefully monitored until they fully recovered from anesthesia before they were returned to their home cage. The monkeys received antibiotics (ceftiofur sodium; 2.2 mg/kg, intramuscular; every 24 h) and analgesics (buprenorphine; 0.005–0.01 mg/kg intramuscular; every 8–12 h) for 3 days after surgery.

### Microelectrode Mapping

Multi-unit microelectrode recordings were used to characterize neuronal responsiveness, receptive properties, and topography. Surgical procedures for cortical mapping have been fully described elsewhere (Merzenich et al. 1978; Kaas and Florence 1997; Jain et al. 2008; Qi, Chen et al. 2011). Each monkey was

initially sedated by a ketamine injection (10–30 mg/kg, intramuscular), followed by isoflurane anesthesia (1–2%). A craniotomy and durotomy were performed to expose areas 3a, 3b, 1, 2/5, and near the lateral sulcus for S2 and PV. The anesthesia was switched to intravenous infusion of ketamine hydrochloride (12 mg/kg/hr) for neuronal recordings. A low impedance tungsten microelectrode (1 M $\Omega$ , Microprobes) was inserted perpendicularly into the cortex with a hydraulic micromanipulator (Narishige International USA), and placed in ~300  $\mu$ m spacing with allowances for blood vessels. In areas 3a, 3b, 1, and 2/5, the microelectrode was held between 25–40° off the vertical plane. Recording angle in areas S2/PV was 40° off the vertical plane for most of the cases.

Multi-neuronal responses were constantly evaluated as the microelectrode passed through the layers of somatosensory cortex (up to 1000  $\mu$ m in depth). To access the S2 and PV regions, we made deep penetrations from the brain surface (typically starting from the area 3b face region) up to 5000–6000  $\mu$ m, where no response was encountered. Since we found that the cortex usually did not respond to tactile stimulation at or beyond the depth of 2000  $\mu$ m below the pia surface, we designated the recording sites at or above the depth of 1900  $\mu$ m to areas 3b, or 3a or 1 based on the locations of the penetrations in the reconstructed map. Recording sites at the depth of 2000  $\mu$ m or deeper were considered to be areas S2/PV.

For each penetration at the site where the strongest evoked response occurred, we characterized the neuronal RF location, size, and response preference to somatosensory stimuli. Neuronal responses were classified as "cutaneous" when evoked by light contact on the skin or hair movement, "high threshold" when required taps to the skin, and "non-cutaneous" when only responsive to joint and muscle manipulation. The minimum RF was determined to be the area of skin where light touches with a hand held probe activated the recorded neurons (Merzenich et al. 1978). At the end of the recording sessions, electrolytic lesions were made by passing anodal direct current (10  $\mu$ A) at strategic locations for later alignments of recording results to cortical architecture from histological tissue processing.

## Subcutaneous Digit Injections

To determine the spinal cord lesion level and extent, we subcutaneously injected a transganglionic transport tracer cholera toxin subunit B (1% CTB, Sigma) or CTB conjugated to wheat germ agglutinin-horseradish peroxidase (0.2% BHRP, List Biological) into the distal phalanges of digits 1, 3, and 5 of both hands, 4–7 days prior to the electrophysiological experiment. See details in Qi, Chen et al. (2011)

## Tissue Processing and Histology

Following the terminal mapping experiment, each monkey was euthanized with a lethal dose of pentobarbital (120 mg/kg). Once areflexive, the monkey was perfused transcardially with phosphate buffered saline (PBS, pH 7.4), followed by 2–4% paraformaldehyde in 0.1 M phosphate buffer (PB), and subsequently 10% sucrose-containing fixative. The brain and spinal cord were removed, immersed in 30% sucrose in PB, and refrigerated overnight. The spinal cord of 12 cases was cut at 40  $\mu$ m in the horizontal plane, and 1 case (SM-RO) was cut at 50  $\mu$ m in the transverse plane. The lower brainstem was cut at 40  $\mu$ m in the transverse (coronal) plane, and the cortex was cut in the tangential plane for nine monkeys and in the coronal plane for four monkeys.

In monkeys with the subcutaneous CTB injections, tissue was processed to reveal transported CTB tracers (see Qi, Chen et al. 2011 for details). In short, 1:4000 dilution of goat anti-cholera toxin subunit B (List Biological Labs), 1:200 dilution of biotinylated rabbit anti-goat IgG (Vector Laboratories PK-4005), and a Vectastain ABC kit (Vector Laboratories PK-4005) and a Vector VIP substrate kit (Vector Laboratories SK-4600) were used to show the labeling in pink/purple color. In the case (SM-W), BHRP was used as a neuroanatomical tracer, and tetramethylbenzidine (Gibson et al. 1984) reaction was used to reveal labeled terminal fields in the brainstem and spinal cord. For the cortex, every third section was processed for cytochrome oxidase (CO, Wong-Riley 1979), myelin (Gallyas 1979), or vesicular glutamate transporter 2 (VGLUT2) for architectonic analysis (see Qi, Gharbawie, et al. 2011 for details).

## Electrophysiological Map Reconstruction

The hand representation in somatosensory cortex was reconstructed by relating RFs to corresponding recording sites in Adobe Illustrator CS6 (Adobe Systems, San Jose, CA). See Qi, Chen et al. 2011 for details. The reconstructed electrophysiological maps in areas 3a, 3b, 1, and 2/5 were carefully superimposed on the images of brain sections processed for architectural markers (e.g., myelin, CO, VGLUT2, and CTB) by using small electrolytic reference lesions and other landmarks (e.g., central sulcus (CS)) for alignments. For the deep penetrations in cortex of the upper bank of lateral sulcus, a similar strategy was used to construct a surface view of the cortex of the unfolded lateral sulcus. The positions of the reference lesions, the orientations of the electrode tracts, and the locations of the labeled neurons from tracer injection in area 3b (in some monkeys) were considered. A step-by-step illustration demonstrates how the electrophysiological map from S2/PV was reconstructed (Supplementary Fig. S1). Note that even though we attempted to be as precise as possible in reconstructing the map of recording sites, small uncertainties remain due to tissue distortion from flattening the cortex and the angle of the microelectrode passing through cortical columns in areas S2/PV.

## Determining Boundaries of Somatosensory Areas 3a, 3b, 1, 2/5, and S2/PV

We used standard architectonic and electrophysiological mapping methods to define areal boundaries of the somatosensory cortex (Carlson et al. 1986; Krubitzer and Kaas 1990). However, when the DCL was severe, such that the majority of neurons in somatosensory areas were unresponsive or response patterns were altered, we primarily relied on the architectonic criteria to estimate areal boundaries. Area 3b more densely expresses CO, myelin, and VGLUT2. The established widths of hand regions of areas 3b and 1 were also considered (e.g., Merzenich et al. 1978; Kaas et al. 1979; Sur et al. 1982).

The squirrel monkey has a shallow central sulcus, and defining areal boundaries by recordings near this sulcus presented challenges. Based on the response patterns of neurons in the current cases and those in an earlier study (Sur et al. 1982), we designated recording sites from the pia surface to a depth of 1290  $\mu$ m along the anterior bank of CS to area 3a, and recording sites between 1300  $\mu$ m to 2800  $\mu$ m to area 3b. Beyond 2800  $\mu$ m, we usually recorded no response, presumably because the microelectrode entered the white matter. Recording sites along the caudal bank of the CS between 1300  $\mu$ m to 2800  $\mu$ m below the pia surface were considered to be in area 3b. These distinctions agree well with the architectural boundaries.

The somatosensory areas S2 and PV are architectonically less distinct in histological preparations (Krubitzer and Kaas 1990; Qi et al. 2002; Coq et al. 2004). Nevertheless, with the guidance of strategically placed electrolytic lesion markers, we were able to overlay reconstructed microelectrode maps on images of the flattened cortex sections. This was completed for nine monkeys, as the cortex in the other four monkeys was cut coronally. Overall, the S2/PV region was located just lateral to the area 3b face region, but was mostly embedded in the upper bank of the lateral sulcus. The contralateral body was represented head to toe in a mediolateral sequence, and the arm and shoulder were represented in both rostral (PV) and caudal (S2) locations in relation to the joined hand regions in the center of S2/PV (Cusick et al. 1989; Krubitzer and Kaas 1990; Coq et al. 2004). Since it was not possible to draw an exact border between the S2 and PV representations due to reorganization and incomplete reactivation after the DCL, we refer to the region as areas S2/PV.

## Quantitative Analysis

### Evaluating the Extent of the Spinal Cord Lesion

We quantified and compared the areal sizes of labeled axonal terminals in the cuneate nucleus ipsilateral and contralateral with the DCL to better estimate the sparseness of hand inputs in the first relay station (brainstem) after the lesion. ImageJ software (NIH) was used to measure the areal size of CTB label in the cuneate nucleus across rostrocaudal sections, and the total labeled areal size was summed for both sides. The lesion extent was estimated to be the percent of the areal reduction on the lesioned side (see Qi, Chen et al. 2011 for more details). The lesion extents were also estimated from reconstruction from serial horizontal sections of the spinal cord into the transverse view, and there were comparable agreements in the two estimates. However, the quantitative density measures of labeled areas were considered to be more accurate.

### Quantitative Comparisons

We compiled data obtained from areas 3b, 1, and S2/PV for each case, assigned values to independent variables, and



devised a coding scheme to represent variables of interest. Data from areas 3a and 2/5 were not included in the quantitative comparison as these areas were less explored.

To investigate neuron responses to stimulation on the hand and to reduce the data dimensions, we coded a 6-level variable to correspond to the response field size. The value “1” was assigned to a small field restricted to one digit or palm pad, while “6” represented the largest field that included any parts of the hand, arm, and face. The response strength was immediately categorized qualitatively as no response (NR), very weak, weak (WR), or good response (GR) during the mapping session. We then calculated the proportions of responding penetrations within each somatosensory area of each subject, for the categories of response field size and response strength. For some analyses and graphics, this 18-level variable of response strength and RF size was reduced to 12 levels by combining the response strength categories of “very weak” and “weak”. Due to the expected differences in RF sizes between cortical somatosensory areas, we also calculated the proportions of penetrations with WR and GR responses to the hand without regard for RF size as follows:  $WR/(WR + GR)$  and  $GR/(WR + GR)$ . To capture the expected differences in responsiveness due to the lesion severity, we calculated the proportion of penetrations with no tactile responsiveness (NR) within the map of each cortical area:  $NR/(NR + WR + GR)$ .

Data were imported into statistical software (IBM-SPSS 24) for analysis and graphics. Graphics used the response proportions that were calculated for individual monkeys, shown summarized across conditions. Nonparametric Mann–Whitney *U* and Kruskal–Wallis tests were used to assess differences in the distributions of response proportions. The factors considered were: the completeness of the DCL (100%–98%, or <98% complete), recovery time, cortical area, reaching task condition, and exposure to electrical stimulation (ES) of the hand. The recovery times used here (150 or more days of recovery time, or <150 days after the effective lesion) are based on commonly used terms for patients with SCI (e.g., Rowland et al. 2008). The injury phase has been defined by Rowland et al. (2008) by time after SCI. Injury  $\leq 2$  h is primary, immediate phase,  $\leq 48$  h is early acute phase,  $\leq 14$  days is secondary subacute phase,  $\leq 6$  months is intermediate phase, and  $\geq 6$  months is chronic/late phase. We examined the correlation of the percent of responses to the hand between different cortical areas as an indicator of similarity of recovery after DCL.

## Results

The primary goals were (1) to characterize the response properties in the hand regions of higher-order somatosensory areas S2/PV, and 2/5 (if obtained), after weeks to months of recovery from contralateral DCL, and to compare those response patterns with other somatosensory areas 3a, 3b, and 1; and (2) to evaluate the impact of lesion extents and post-lesion recovery times, and possible role of interventions on the response properties in these areas. Some of the results from recording in areas 3b and 1 have been fully described in other published studies (Qi, Chen et al. 2011; Chen et al. 2012; Liao et al. 2016, 2018; Qi et al. 2016). For comparison purposes, we have included some of these results in supplementary figures that have been modified from the original published figures with citations. A total of 9164 mapping sites were collected from 13 monkeys. Among those, 446 were in area 3a, 3512 in 3b, 1186 in area 1, 144 in areas 2/5, and 3876 in S2/PV. All recording results from areas S2/PV, illustrations of RFs, and data collected from monkeys SM-H and SM-G are original. For most of the cases we

were able to anatomically verify the locations of the hand region in areas 3b and S2/PV by superimposing the reconstructed microelectrode map on tangentially cut cortical sections processed for CO, CTB, myelin, or VGLUT2. The RF sizes representing the hand varied by area as expected, such that S2/PV and area 2 were ranked as having the largest RFs, followed by area 1, 3a, and 3b, respectively ( $\chi^2 = 94.351$ ,  $df = 4$ ,  $N = 1481$ ,  $P = 1.57 \times 10^{-19}$ ; Fig. 1).

## The Effects of the Completeness of the DCL and the Recovery Time on Cortical Reorganization

We divided the 13 monkeys into four groups based on completeness of DCL and recovery times (Table 1): (1) intermediate recovery times with incomplete lesions ( $n = 4$ ); (2) long-term recovery times with incomplete lesions ( $n = 3$ ); (3) intermediate recovery times with complete or nearly complete lesions ( $n = 3$ ); and (4) long-term recoveries with complete or nearly complete lesions ( $n = 3$ ). Here, we present these results in four subsections, starting with the group with the least severe lesions and the shortest recovery times, followed by groups with more severe lesions and longer recovery times.

### Intermediate-term Recovery with Incomplete DCL

Four squirrel monkeys (SM-A, SM-H, SM-D, and SM-GE) received incomplete unilateral DCL (41%, 64%, 77%, and 79% complete, respectively). The lesion was made at C4 in SM-A, and at the gap between C4 and C5 in SM-GE, to partially deprive inputs from the hand (Supplementary Fig. S2). The DCL in SM-D and SM-H were at C5–C6 to deprive most of inputs from digits 3–5; however, some of the inputs from digit 2 might also be affected. Inputs from the face, parts of the arm, and shoulder were intact in all four monkeys. For each monkey, neuronal responses from both primary and higher-order somatosensory cortex contralateral to the DCL were mapped after 56–142 post-lesion days (Table 1). Among these, three monkeys (SM-A, SM-H, and SM-GE) were not trained or tested on the behavioral task, but SM-D underwent non-intensive testing. Monkeys SM-A and SM-GE received electrocutaneous stimulation of the digits for an fMRI study (see Methods in Qi et al. 2016).

In monkey SM-H that had a 64% complete DCL for 142 days (Fig. 2A), the somatotopy and responsiveness in the hand region of area 3b resembled the normal pattern (Merzenich et al. 1978; Sur et al. 1982). Digits 1–5 were represented in a lateromedial progression with distal digits located rostrally, and proximal digits and palm caudally (Fig. 2B). Neuronal RFs in the mostly spared representations (e.g., digits 1–2, radial palm) were small and restricted to part of digits and palm, which were comparable with those of a normal monkey (Fig. 1, panels SM-H and SM-G). However, neural RFs recorded from the likely deafferented hand region (i.e., digits 3–5, and ulnar palm) were generally large, involving multiple digits and palm pads. Unlike normal monkeys, some neurons had RFs on both dorsal and glabrous sides of hand. Neurons in the hand regions of areas 3a and 1 were less responsive to touch on the hand when compared with those of area 3b.

Neurons in the expected hand region of areas S2/PV responded well to touch on single or multiple digits (Fig. 2C). Representations of forelimb were found rostrally (presumably PV) and caudally (presumably S2) to the hand representation of S2/PV. We did not find responses to touch on the face in the expected hand region of areas S2/PV. However, the somatotopy of the hand region was somewhat disorganized. The response strength to touch on the hand in areas S2/PV was comparable

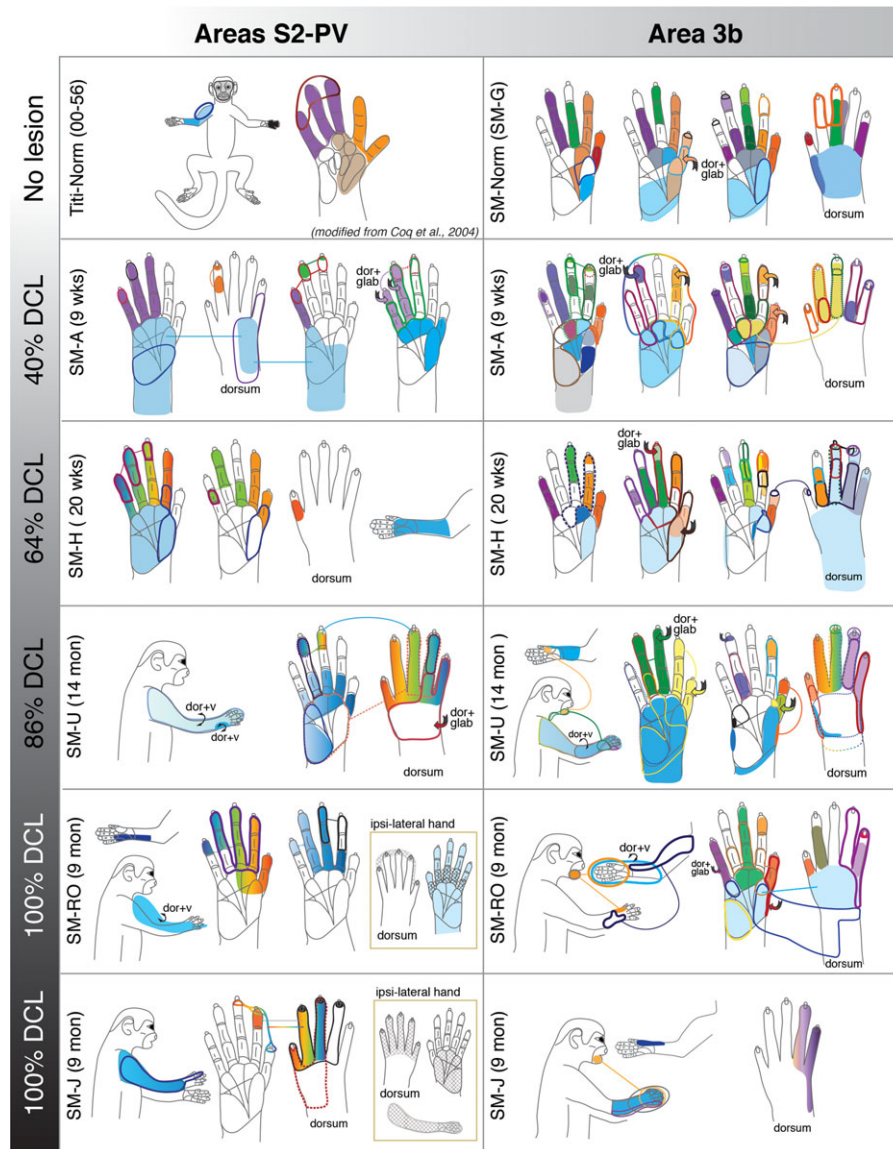


**Figure 1.** Schematic drawings of representative neuronal receptive fields determined from microelectrode recordings in areas 3b and S2/PV. The location and size of receptive fields are color-coded and outlined on drawings of the face, body, and glabrous and dorsal surfaces of the hand. Note that the purpose of this illustration is to depict overall differences in receptive field locations and sizes across monkeys with different dorsal column lesion (DCL) extents and recovery times. Abbreviations: dor+glab, dorsal hair/skin and glabrous skin; dor+v, dorsal and ventral (hair/skin).

to area 3b neurons, and RF properties were similar to the normal pattern (Fig. 1). Despite slight variations between four monkeys in this group, their somatotopy, responsiveness, and neuronal RF sizes in areas 3a, 3b, 1, and S2/PV were similar (Supplementary Figs S3 and S4) to those described for SM-H. We only identified some neurons responsive to touch on the hand in areas 2/5 in monkey SM-GE (Supplementary Fig. S4).

In summary, after incomplete DCL and intermediate recovery times, neurons in the hand regions of S2/PV responded to touch on digits and the hand, and the strengths of responses were comparable to those of area 3b. However, somatotopy was less organized. The degree of cortical reactivation did not seem to vary within intermediate recovery times that ranged between 56 and 142 days. Results from the four monkeys in this group showed that the presence of neurons in areas S2/PV with single digit RFs was usually concurrent with the presence of neurons with single digit RFs in area 3b.

#### Long-term Recovery with Incomplete DCL

Three squirrel monkeys (SM-T, SM-Y, and SM-U) received incomplete DCL (61–86%) at slightly lower levels (i.e., C5–C6) of cervical spinal cord and recovery times ranged from 292 to 414 days (Table 1). Such lesion allowed some inputs from digit 1 and possibly digit 2 to be spared, and inputs from digits 3–5 were partly or mostly deprived. Inputs from the face, arm, and shoulder remained intact. Monkeys SM-Y and SM-U experienced intensive behavior training, and SM-T underwent non-intensive testing. Since reactivation patterns in three monkeys were slightly different due to the lesion level, behavioral training, and recovery time, here we described results by case.

Monkey SM-T had a 61% complete DCL with long-term recovery (Fig. 3A). The somatotopy, neuronal responsiveness, and RF sizes of neurons in areas 3b and 1 resembled those of normal monkeys (Supplementary Fig. S5A). The representation of forelimb in S2/PV was located in the upper bank of lateral

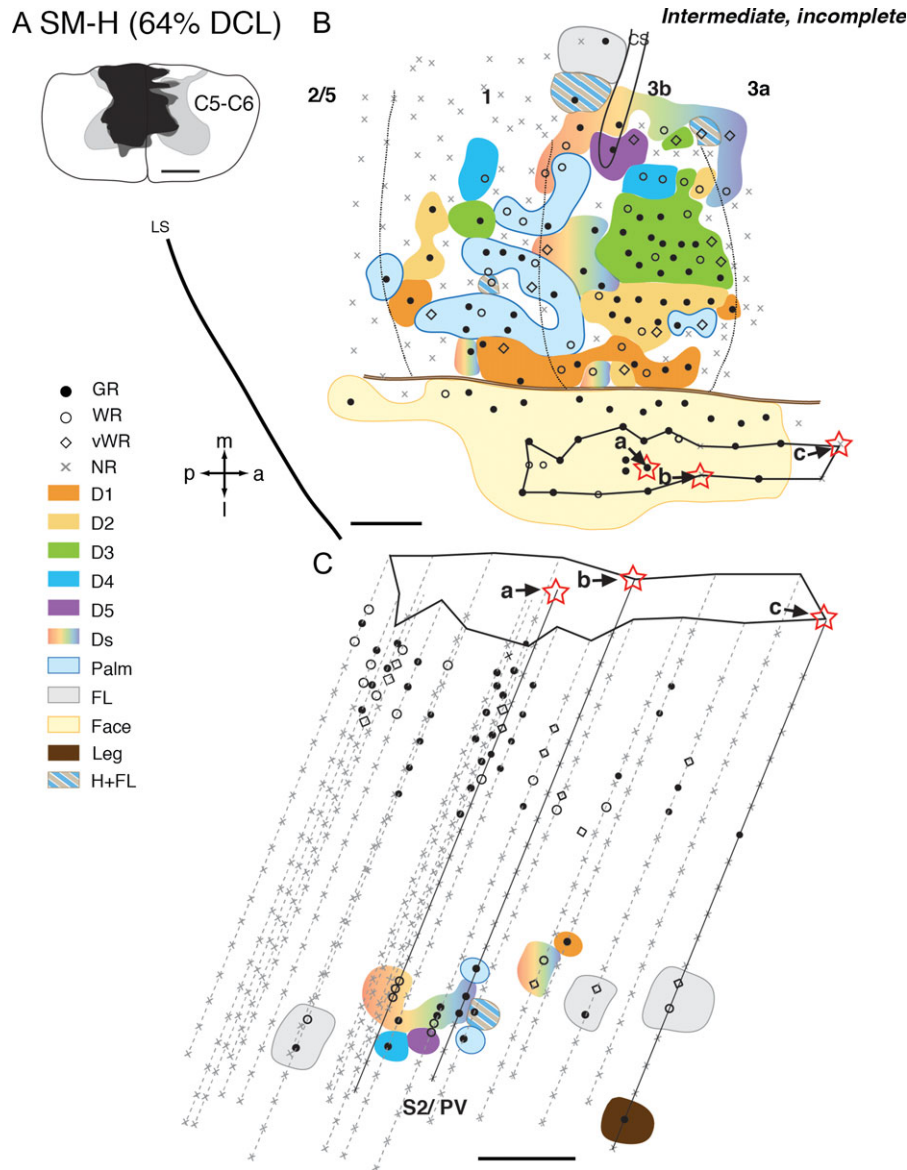


**Figure 2.** Representative case for Group 1. Somatotopic maps of areas 3b, 1, and secondary somatosensory cortex (S2)/parietal ventral (PV) of squirrel monkey SM-H after an intermediate-term, incomplete DCL (64% complete; 142 days) at the C5–C6 level. **A.** Drawing shows the reconstructed transverse view of DCL in the spinal cord. Black shading depicts the area of tissue loss, dark gray surrounding the black shading depicts the area with abnormal tissue, and the light gray depicts the gray matter of the spinal cord. **B.** The reconstructed somatotopic map shows that neurons in hand region of area 3b responded well (shown in solid circle) with a nearly normal somatotopy. The hand region in area 1 is slightly less responsive. **C.** The reconstructed somatotopic map of the hand region in areas S2/PV obtained from deep penetrations. Responses to touch on single digit, multiple digits, or larger areas involving the arm and hand were found between the representations of arm and shoulders that are located rostrally (presumably PV) and caudally (presumably S2). Each symbol (i.e., solid circle, circle, diamond, and x) depicts the location and neuronal responsiveness of one mapping site. Red stars mark the locations of electrolytic lesions made along those electrode penetrations. Neuronal receptive fields in the body parts are color-coded, and color-coded stripes mark combinations of receptive fields in different body parts. Abbreviations: 3a, 3b, 1, 2/5, S2/PV, areas 3a, 3b, 1, 2/5, and S2/PV; a, anterior; C5–C6, cervical segments of C5–C6; CS, central sulcus; D1–D5, digits 1–5; Ds, multiple digits; FL, forelimb; GR, good response; H, hand; H + FL, hand and forelimb; l, lateral; LS, lateral sulcus; m, medial; NR, no response; p, posterior; vWR, very weak response to hard taps; WR, weak response; Scale bar is 1 mm in A, B, C.

sulcus, and at the same rostrocaudal location of area 3b face region (Fig. 3B). The forelimb region of S2/PV was confirmed with strategically placed electrolytic lesion markers (“c” and “d”). The superimposed electrophysiological map of S2/PV onto the CTB section indicated that the forelimb region was near the labeled neurons and terminals after tracer injection into the digit 2 representation of area 3b. The hand representations of S2/PV were roughly located between the rostral forelimb region (likely area PV) and caudal forelimb region (likely

area S2), resembling the normal somatotopy. We found that neurons in the expected hand region of S2/PV responded well to touch on single or multiple digits, palm pads, and the hand and forelimb, and occasionally on glabrous and dorsal surface of digits (Fig. 3C). These patterns were similar to those of normal New World monkeys (e.g., Cusick et al. 1989; Coq et al. 2004).

Monkey SM-Y had a complete DCL but at a slightly lower level (C5–C6), hence the inputs from digit 1 and possibly digit 2



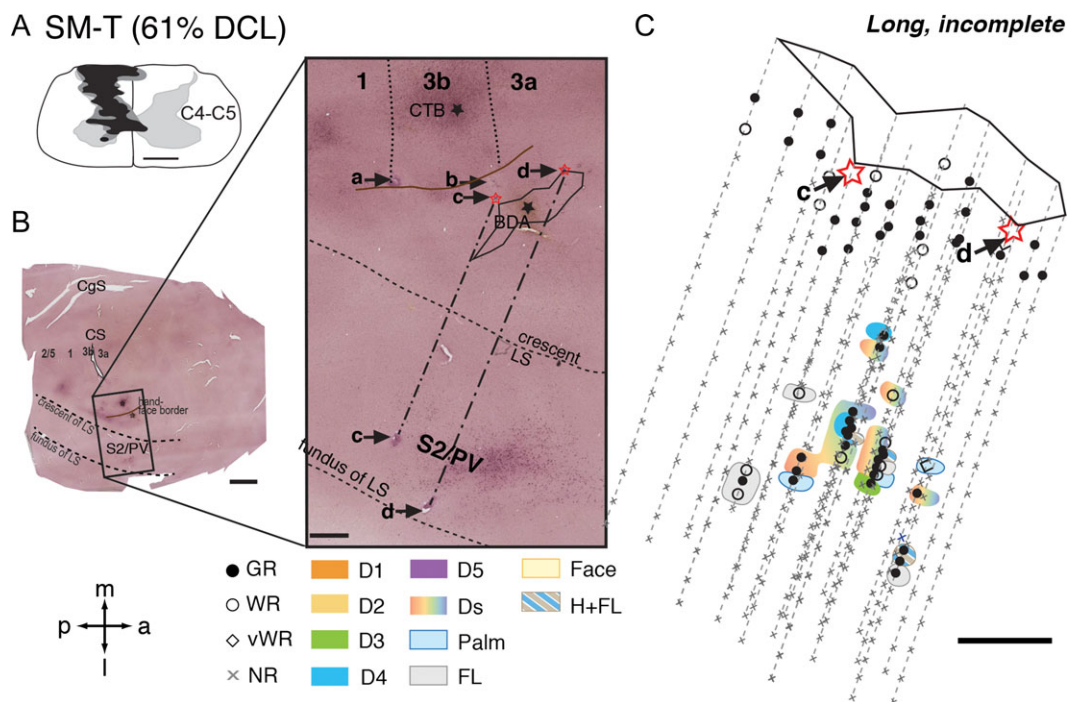


**Figure 3.** Representative case for Group 2. Alignment of the somatotopic map of areas S2/PV and brain sections stained for cholera toxin subunit B (CTB) in monkey SM-T after a long-term, incomplete DCL (61% complete; 321 days) at the C4–C5 level. **A.** Drawing shows the reconstructed transverse view of DCL in the spinal cord. **B.** Photomicrographs of flattened cortical sections immunoreacted for CTB labeling showing CS, unfolded LS, and locations of strategically placed electrolytic lesions of a, b, c, and d. Among these, “c” and “d” are deep microelectrode penetrations inserted from the pia surface in the face region of area 3b into the hand region in S2/PV in the upper bank of lateral sulcus. **C.** The reconstructed somatotopic map shows responses encountered from deep penetrations recorded in areas S2/PV. Scale bar is 5 mm in the low magnification image of panel B (left), and is 1 mm in all others. Abbreviations: C4–C5, cervical segments of C4–C5; CgS, cingulate sulcus. Other conventions follow Figure 2.

were spared (Supplementary Fig. S2). This monkey was intensively trained to use the impaired hand for the reach-to-grasp task. As described in our early study (Liao et al. 2016), large-scale reorganizations in the hand regions of areas 3b and 1 were found (Supplementary Fig. S6). The representations of spared digits 1 and 2 were abnormally large. The digit 1 representation expanded to, or even beyond, the expected territory of digit 4, suggesting that the spared digit 1 inputs directly or indirectly activated the deprived hand cortex.

Again, we found that the forelimb representations of S2/PV were located in the upper bank of lateral sulcus near the labeled foci after CTB injection into the digit 2 representation of area 3b. The hand region was roughly located between the rostral and caudal representations of the forelimb, resembling the normal somatotopy. Although many deep microelectrode penetrations were made into this region, we only found few recording sites that responded well to touch on multiple digits, digit and palm pads, dorsal and glabrous digits, or hand and forelimb. Most of the mapping sites were unresponsive.

The third monkey SM-U had an extensive DCL (86% complete) with longer survival time (414 days), and the impaired hand was intensively trained on the reach-to-grasp task. As indicated in our early publication (Liao et al. 2016), areas 3b and 1 underwent large-scale reorganizations (Supplementary Fig. S7) including sites highly responsive to touch or taps on digits, hand, or on both hand and forelimb. Many neurons had abnormally large RFs involving glabrous and/or dorsal sides of the entire digit, multiple digits, large portion of palmar pad, or combinations of hand and forelimb, and occasionally hand and face (see Fig. 1 for representative examples).

In areas S2/PV, some neurons responded well to touch on the partially denervated hand, but more than half of neurons responded weakly. Overall, the strengths of neural responses to touch on the hand were generally weaker than those to touch on the forelimb alone or on the forelimb and hand together. Somatotopy was similar to that of SM-T and roughly resembled the normal pattern, in which the arm and shoulder representations in PV and S2 were separated by the representations of digits and hand in between. Neuronal RFs were usually large except in a few mapping sites responsive to touch on digit 4 (Supplementary Fig. S7C). Most neuronal RFs involved glabrous and/or dorsal sides of hand, multiple digits, digits and palm, or combination of hand and forelimb (Fig. 1). Both areas 3a and 2/5 were responsive to touch or taps on the digits and palm, but the responsiveness was weaker in areas 2/5.

In summary, primary and higher-order somatosensory areas were reactivated after incomplete DCL with long-term recovery times. The reactivation patterns varied depending on the level and the extent of DCL, and whether monkeys were intensively trained to use to the impaired hand.

#### Intermediate-term Recovery with Complete or Nearly Complete DCL

Three squirrel monkeys (SM-BB, SM-C, and SM-O) were evaluated 48–131 days after receiving nearly complete unilateral DCL (98%, 98%, 99%, respectively). In monkeys SM-C and SM-O, DCL at the C4 level deprived most of the inputs from hand. Monkey SM-BB had a nearly complete DCL (98%) at C5 that spared some inputs from digit 1 and the radial palm, but deprived inputs from digits 2 to 5. All inputs from the face and most of the inputs from the arm and shoulder remained intact in all three



monkeys. Monkey SM-BB was not behaviorally trained and not tested but received electrocutaneous stimulation of digits as part of the fMRI study of Qi et al. (2016). Monkeys SM-C and SM-O underwent non-intensive testing on the reach-to-grasp task.

In monkey SM-BB, neurons in the expected digit 1 territory of areas 3b and 1 responded well to touch on the digit 1 and radial palm (thenar pad, PTH), but the mostly deprived cortex (expected representations of digits 2–5) was less responsive to touch or taps on hand (Qi et al. 2016; see Supplementary Fig. S5B). Some neurons in the hand region of S2/PV responded to touch or light taps on multiple digits, palm, or combinations of hand and forelimb/ shoulder (Fig. 4). Surprisingly, we also found many neurons responding well to touch within small RFs restricted to single digits 1, 3, 4, and 5 (Fig. 4C).

In monkeys SM-C and SM-O, scattered sites in the hand region of area 3b responded to touch on digits 1–5 in a nearly normal somatotopy, although neurons in the expected palm representation remained unresponsive (Supplementary Figs S8 and S9). Neurons were less responsive in areas 3a, 1, and 2/5 in these two monkeys. In monkey SM-O, neurons in the forelimb region of areas S2/PV were generally not responsive (Supplementary Fig. S8). Neurons in few recording sites responded to touch on hand, forelimb, upper trunk, and occasionally on large areas involving hand and face, or bilateral forelimbs. In monkey SM-C, although some neurons responded well to peripheral stimulation in the forelimb region of areas S2/PV, the somatotopy was abnormal and largely disorganized. Besides a few sites where neurons responded to touch on multiple digits, most reactivated neurons in the hand region had large RFs involving the hand and the rest of the forelimb, or arm and shoulder (Supplementary Fig. S9).

Area 3a was much less responsive in all three monkeys, and areas 2/5 were partially responsive to touch on digits in SM-BB, SM-C, and SM-O, but were not fully explored (Fig. 4, Supplementary Figs S8 and S9).

In summary, in monkeys with severe DCL and intermediate times of recovery, neurons in the deprived hand regions of primary and higher-order somatosensory areas were responsive to touch on the hand in a roughly somatotopic pattern. However, in two monkeys that had DCL at a higher level in the spinal cord (C4), neurons in the hand region of S2/PV were either not fully responsive, or responded to touch or taps mostly to the forelimb alone, rather than to forelimb in combination with the hand. In contrast, in SM-BB after DCL at a lower level (C5) and after electrocutaneous stimulation on the digits, the hand regions of areas 3b and S2/PV were highly responsive to touch on single or multiple digits.

#### Long-term Recovery with Complete or Nearly Complete DCL

Three squirrel monkeys (SM-RO, SM-W, and SM-J) received complete or nearly complete DCL (estimated 100%) at a higher cervical level (C4) that interrupted inputs from the entire hand, but inputs from face, arm, and most of the shoulder were preserved. Neuronal responses were examined following 253–285 days of recovery. Note that monkey SM-J experienced intensive training and SM-RO underwent non-intensive testing. SM-W was not behaviorally trained or tested, and the affected forelimb was severely impaired throughout the entire post-lesion time. The hand regions in areas 3a, 3b, 1, and S2/PV in all three monkeys were verified histologically. Parts of the results for the reorganized somatotopic maps in area 3b have been published (Liao et al. 2016, 2018).

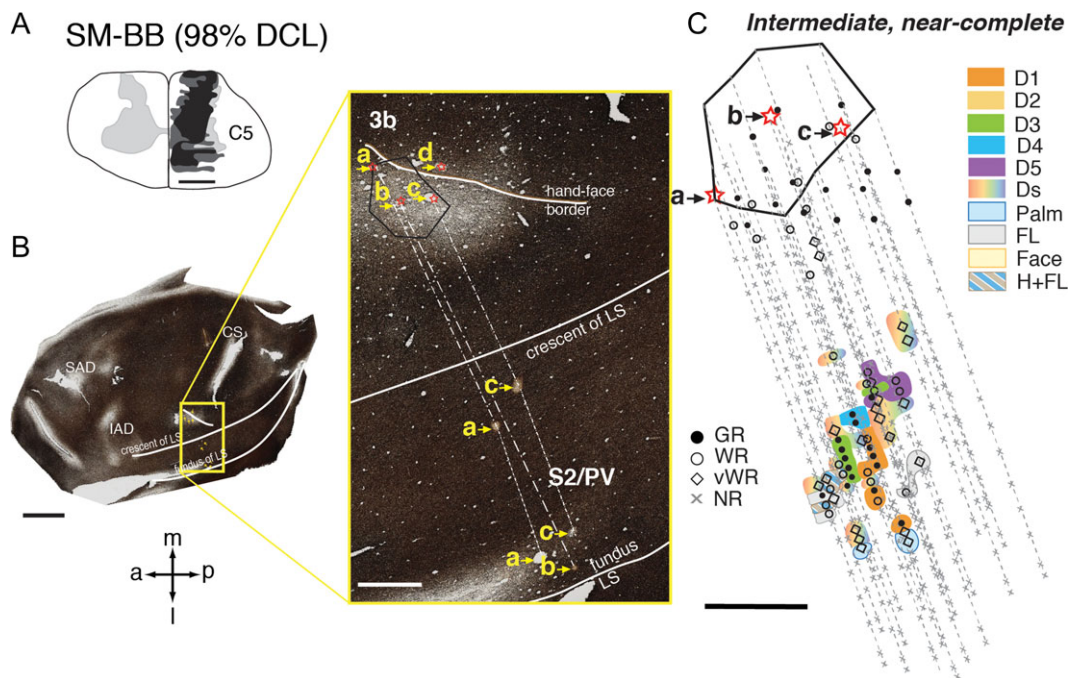


**Figure 4.** Representative case for Group 3. Alignment of the somatotopic map of areas S2/PV and brain sections stained for myelin in monkey SM-BB after an intermediate-term, near-complete DCL (98% complete; 49 days) at the C5 level. **A.** Drawing shows the reconstructed transverse view DCL in the spinal cord. **B.** Photomicrographs of a flattened and myelin stained section through somatosensory cortex showing the landmarks and locations of strategically placed electrolytic lesions of a, b, c, and d (marked with red stars and yellow arrows). Among these, “a”, “b”, and “c” are deep microelectrode penetrations inserted into the hand region of areas S2/PV in the upper bank of lateral sulcus. **C.** The reconstructed somatotopic map shows responses encountered from deep penetrations recorded in areas S2/PV. Abbreviations: IAD, inferior arcuate dimple; SAD, superior arcuate dimple. Scale bar is 5 mm in the low magnification image of panel B (left), and 1 mm in all others. Other conventions follow Figure 2.

In monkey SM-RO, as briefly described in Liao et al. (2018), neurons in more than half of the mapped sites in the hand region in area 3b remained unresponsive to touch or taps (Supplementary Fig. S5C). However, we found scattered mapping sites where neurons responded weakly to light taps on single digits 1, 2, 4, and 5 with a roughly normal lateromedial sequence along the rostral border of area 3b. Somatotopy, neuronal responsiveness, and RF sizes in the hand region of area 1 resembled the response pattern of area 3b. This reactivation of areas 3b and 1 in SM-RO suggested that a few undetected spared axons might have survived the cut and restored the hand responsiveness in somatosensory cortex. In areas S2/PV, we found scattered neurons responsive to touch or taps on the face, digits and hand, forelimb, trunk, and hindlimb from 53 deep penetrations (Fig. 5). The majority of mapping sites in the expected hand region were either unresponsive or responded weakly to hard tapping on the hand. Note that neurons outside the affected hand region responded well to touch on the face, arm or shoulder, trunk, and hindlimb, indicating that the less responsive hand region of S2/PV was due to the specific deafferentation.

In monkey SM-W, area 3b underwent large-scale reorganization. Instead of responding to touch/taps on the hand, many neurons in the deprived hand regions responded to touch or taps on the face, forelimb, or the combination of the face and forelimb (Supplementary Fig. S10). Somewhat differently, intensive trained monkey SM-J had more neurons in the deprived hand region of area 3b responded to touch or taps on the hand (Supplementary Fig. S11). These observations suggested that the intensive training might restore some cortical activation in area 3b along with hand function after nearly complete DCL. Neurons in area 1 were largely unresponsive in these two monkeys, regardless of the behavioral intervention. Similarly, the somatotopy in the deprived hand region of areas S2/PV of both monkeys was highly abnormal. Many neurons became

responsive to touch on the arm and shoulder, face, or the hand and face. Surprisingly, the responsiveness of neurons with RFs involving the hand was stronger than that in area 3b.

Neurons in deprived hand regions of area 3a in these three cases were primarily unresponsive to touch and taps on the hand, although neurons in the intact forelimb regions responded well to touch or taps on the forelimb. In two monkeys (SM-W and SM-J) for which areas 2/5 were explored, neurons were mostly unresponsive to touch or taps on the hand and arm (Supplementary Figs S10 and S11).

In summary, nearly half of the recording sites in the deprived hand regions of area 3b, and most sites in 3a, 1, and 2/5, neurons were not responsive in all three monkeys. Somatotopy and neuronal RF locations and sizes of deprived hand regions of area 3b varied greatly from normal. Although the response patterns in primary somatosensory area 3b were different between the three monkeys, the reactivation patterns between area 3b and higher-order somatosensory areas S2/PV within the same monkeys were strikingly similar. Surprisingly, in all three monkeys we encountered some neurons in S2/PV that had stronger responses to touch on the hand than we encountered in area 3b.

### Neuronal Response Properties Associated with Hand Use Behavior and Electrocutaneous Stimulation after Lesion

Here, we examined if intensive training or electrocutaneous stimulation benefited somatosensory reactivation after deafferentation from hand in monkeys.

#### Intensive Training Effects

After monkeys recovered from DCL surgery, we closely observed their cage behaviors, such as walking, climbing,

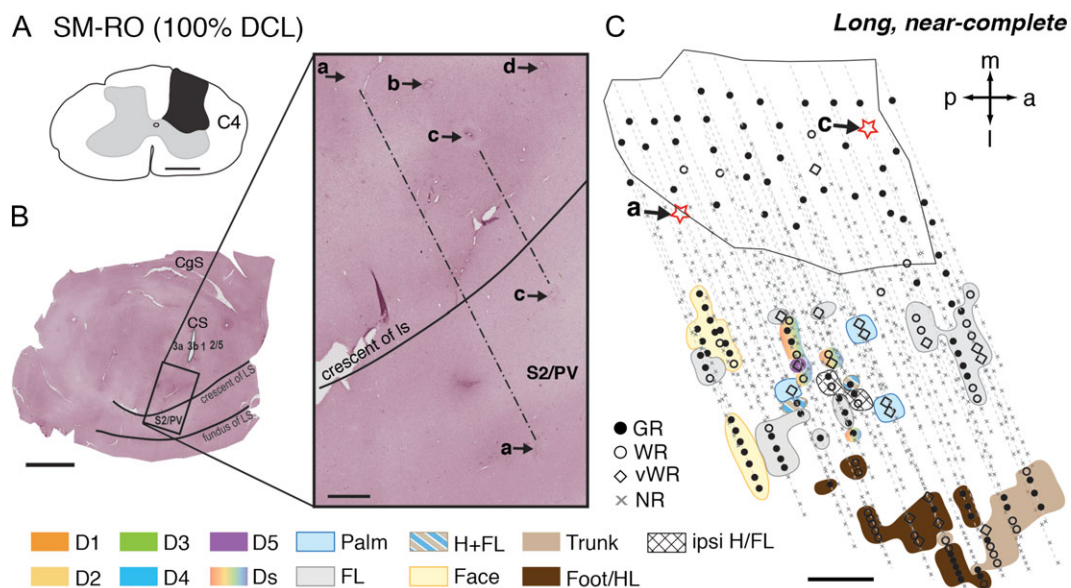


**Figure 5.** Representative case for Group 4. Alignment of the somatotopic map of areas S2/PV and brain sections stained for CTB in monkey SM-RO after a long-term, complete DCL (100% complete; 253 days) at the C4 level. **A.** Drawing shows the reconstructed transverse view of DCL in the spinal cord. **B.** Photomicrographs of a flat-mounted cortical section immunoreacted for CTB labeling showing the landmarks and locations of strategically placed electrolytic lesions of a, b, c, and d (marked with arrows and stars). Among these, “a” and “c” are deep microelectrode penetrations inserted into the hand region of areas S2/PV in the upper bank of lateral sulcus. **C.** The reconstructed somatotopic map shows responses encountered from deep penetrations recorded in areas S2/PV. Scale bar is 5 mm in the low magnification image of panel B (left), and 1 mm in all others. Abbreviation: Ipsi, ipsilateral. Other conventions follow Figure 2.

reaching, or manipulating food items. Immediately after DCL, most monkeys were reluctant to reach for food or manipulate food with their affected forelimb. Hand use progressively improved over post-lesion weeks to month, although the degree of recovery depended on the lesion level and severity. By the time of the final procedure, most of the monkeys showed little to no deficit. However, there were a few exceptions when the DCL was nearly complete to complete.

First, we used two extreme examples to evaluate the relationship between behavior deficit and cortical reorganization. Both monkeys SM-J and SM-W had a complete DCL at C4, and their recovery times were 285 and 266 days, respectively. While monkey SM-J was intensively trained to use the impaired hand, SM-W was neither trained nor tested. SM-J had strong deficits leading up to the final evaluation, but the task performance recovered to a nearly normal level by the final behavioral test. In contrast, SM-W had much stronger deficits in the affected hand, not only for reach and grasp behavior, but also for forelimb walking and climbing through the entire evaluation period. While many neurons in areas 3a, 3b, 1, and 2/5 of these two monkeys remained unresponsive or responded weakly to peripheral stimulation, we found responsive neurons in the deprived hand region in area 3b and S2/PV in monkey SM-J to taps on the glabrous and/or dorsal sides of digits, palm, and forelimbs (Fig. 1, Supplementary Fig. S11). However, the reactivated hand neurons in areas 3b and S2/PV in monkey SM-W became responsive to high-threshold taps on large areas of face and forelimb (Supplementary Fig. S10). This suggested that the intensive training promotes favorable reactivation in the deprived somatosensory cortex, and contributed to the behavioral recovery of hand use.

Second, intensive training may shape the somatotopy in the deprived somatosensory cortex when the DCL was incomplete. In one non-intensively trained monkey SM-T (Supplementary Fig. S5A) and monkeys without the behavior intervention (SM-H, Fig. 2; SM-A, Supplementary Fig. S3; SM-GE, Supplementary Fig. S4), the reactivated somatotopic maps in the partially deprived areas 3b and 1 resembled those of normal monkeys, despite that the responses were somewhat weaker. However, in another two intensively trained monkeys (SM-U and SM-Y) with the incomplete DCL, the hand region of somatosensory areas 3b and 1 underwent large-scale reorganization. The representation of spared digit 1 in area 3b expanded few mm medial into the deprived territory (Supplementary Fig. S6), and unusually large RFs occurred in the hand regions of areas 3b, 1, and S2/PV (Fig. 1, Supplementary Fig. S7). The results suggested that intensive training could reshape the functional map, especially when the DCL was incomplete. However, the restoration of somatotopic map in areas 3b and 1 is limited when the lesion is complete (SM-J, Supplementary Fig. S11).

#### Electrocutaneous Stimulation Effect

Three monkeys (SM-A, SM-BB, and SM-GE) received low (2 mA) and high (4 mA) level electrocutaneous stimulation on distal finger pads of the hand before and 2, 4, and 6 weeks after a unilateral DCL (see details in Qi et al. 2016). All three monkeys showed robust recovery of somatotopy and responsiveness in the primary and higher-order somatosensory areas, despite the varying lesion severities from 40 to 98% complete (Fig. 4, Supplementary Figs S3 and S4). Specifically, we found that more responsive neurons in the somatosensory areas, especially the S2/PV, had smaller RFs (e.g., single digits or palm pads) on the affected hand (Fig. 6) when compared with monkeys without the

electrocutaneous stimulation in the present study. This surprising finding requires further investigation.

#### Quantitative Comparisons

After categorizing penetrations by responsiveness and RF size, we calculated the category proportions for each somatosensory area of each monkey. Summarizing results across monkeys, we compared the proportions of weak and GRs with hand stimulation between areas 3b and 1, and S2/PV (Fig. 7). Because we did not collect large samples from areas 3a, 2, and M1 in all cases, we did not include these areas in statistical analyses.

Using our categorization methods for quantification, hypothesis testing confirmed the expected results that, overall, area 3b had smaller RFs than area 1 ( $H = 87.72$ ,  $df = 2$ ,  $N = 1359$ ,  $P = 1.5 \times 10^{-6}$ ), and area 1 had smaller RFs than S2/PV ( $P = 2.3 \times 10^{-5}$ ). All areas tended to have higher proportions of hand responses with larger RF sizes when the DCL was more complete with longer recovery times ( $H = 102.92$ ,  $df = 35$ ,  $N = 240$ ,  $P = 1.32 \times 10^{-8}$ ). A summary of the hand response proportions by area and category (Fig. 7A) illustrates several tendencies. DCL effectiveness and recovery time affected area 3b, and area 1 to a lesser extent, such that larger proportions of hand responses classified as GR and restricted to a single digit or pad were found in cases after incomplete DCL with intermediate-term recovery times; and the lowest proportions (none, in area 1) were found after complete DCL with long-term recoveries. In S2/PV, RFs restricted to a single digit or pad were found in similar (but low) proportions across DCL conditions, except after long-term complete DCL, in which no cases had single digit RFs in S2/PV (see SM-H and SM-RO in Fig. 1). We also found unexpected differences between areas S2/PV compared with areas 3b and 1 for the relative proportions of large RFs within the hand and large RFs that included the hand along with the arm and/or face. For schematics of RFs in example monkeys after different lesion and recovery conditions, see Figure 1.

Across DCL conditions, broad RF locations were generally consistent across areas within individual cases (Fig. 7B). When comparing RFs across the three areas we quantified, area 3b was the reference because the map was the most complete. Most of the cases had 100% correspondence between the presence of RFs in area 1 and those found in area 3b (10/13), and the presence of RFs in S2/PV and those found in area 3b (9/13). Supplementary Figure S12 shows the detailed correspondence of RF locations for the area maps for each case, from which the percentages in Figure 7B were derived.

When the proportions of weak and good hand responses were considered regardless of RF sizes for each area within each monkey, areas 3b and 1 were similarly affected by the DCL completeness and recovery time (Fig. 7C). The response proportions classified as very weak and weak (WR) tended to be higher, and those classified as GR tended to be lower in cases after (nearly) complete DCL with long-term recovery in area 3b ( $H = 7.824$ ,  $df = 3$ ,  $N = 13$ ,  $P = 0.050$ ) and area 1 ( $H = 7.350$ ,  $P = 0.062$ ). The DCL completeness as a factor alone influenced the response proportions in area 3b ( $U = 39$ ,  $P = 0.010$ ) and area 1 ( $U = 36.5$ ,  $P = 0.027$ ), while the recovery time alone did not ( $P = 0.295$ ,  $P = 0.101$ , respectively). The response proportions in S2/PV did not vary detectably by lesion conditions (DCL and recovery time) considered together ( $H = 1.354$ ,  $P = 0.716$ ) or separately (completeness:  $P = 0.943$ ; recovery time:  $P = 0.295$ ). Overall, the proportions of GR to touch on the hand were ranked significantly higher in S2/PV than 3b ( $U = 567.5$ ,  $N = 83$ ,  $P = 0.009$ ). Area 1 followed a pattern similar to 3b ( $U = 558.5$ ,  $N = 77$ ,  $P = 0.063$ ). These analyses recapitulate our observations of unexpected GRs to the hand in



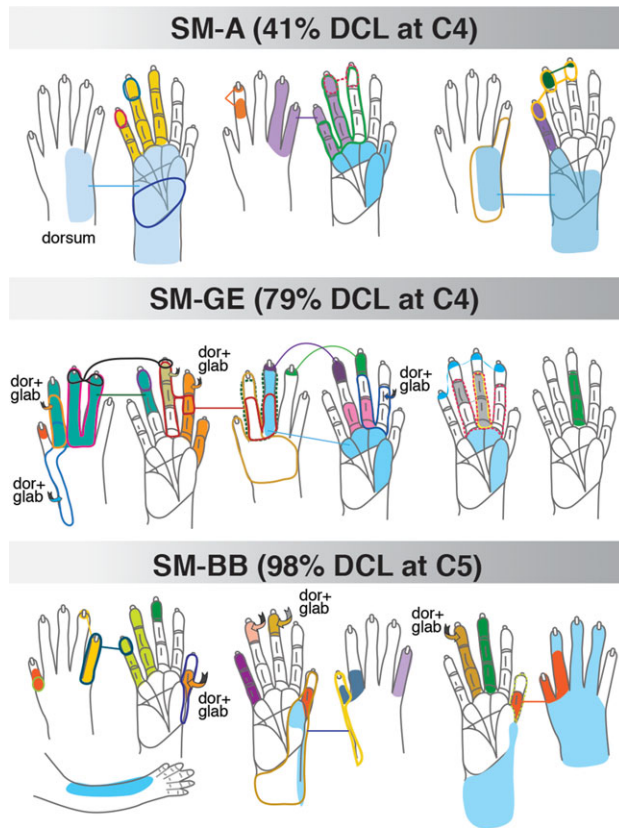


**Figure 6.** Schematic drawings of representative neuronal receptive fields determined from microelectrode recordings in the hand region of areas S2/PV after electrocutaneous stimulation on alternate digits 1–3 at pre- and 2, 4, 6 weeks post-DCL. The location and size of receptive fields are color-coded and outlined on the drawings of the glabrous and dorsal surfaces of the hand and forelimb. Note that the size of receptive fields varies from one digit phalange to almost the entire hand. Other conventions follow Figure 1.

S2/PV when few GRs to the hand were encountered in areas 3b and 1 after a complete DCL.

In a corresponding trend, increased proportions of unresponsive penetrations (NR) in S2/PV were associated with complete DCL and long recovery times (Supplementary Fig. S13). The NR penetrations were tallied from the entire map, but because the mapped regions varied in S2/PV across cases, we focused primarily on properties associated with responses to touch on the hand.

The proportions of hand responses characterized as WR or GR were examined with correlations between cortical areas (Supplementary Fig. S14), which showed that the relationships tended to be strongest between areas 3b and 1. Over all DCL conditions combined, we found GR proportions were positively correlated between areas 3b and 1 ( $\rho = 0.371$ ,  $N = 49$ ,  $P = 0.009$ ); but when assessed separately, a significant correlation was reliably detected only in monkeys after incomplete DCL with long-term recovery ( $\rho = 0.694$ ,  $N = 12$ ,  $P = 0.012$ ). For WR over all DCL conditions, areas 3b and 1 were also positively correlated ( $\rho = 0.483$ ,  $N = 52$ ,  $P = 2.92 \times 10^{-4}$ ). Statistically significant correlations were found between areas 3b and 1 for WR in monkeys after incomplete DCL with intermediate-term recovery ( $\rho = 0.563$ ,  $N = 16$ ,  $P = 0.023$ ) and long-term recovery ( $\rho = 0.869$ ,  $N = 12$ ,  $P = 2.46 \times 10^{-4}$ ), and after complete DCL with long-term recovery ( $\rho = 0.644$ ,  $N = 13$ ,  $P = 0.018$ ). In addition, WR in monkeys after incomplete lesions with intermediate-term recovery

showed correlation between areas 3b and S2/PV ( $\rho = 0.582$ ,  $N = 16$ ,  $P = 0.018$ ) and between areas 1 and S2/PV ( $\rho = 0.521$ ,  $N = 16$ ,  $P = 0.039$ ).

When examining the effects of hand-use training on responses, we did not detect differences in the distributions of the response proportions across categories of behavioral intervention condition ( $H = 3.493$ ,  $df = 5$ ,  $N = 240$ ,  $P = 0.624$ ). There was a tendency for cases with intensive training to be more responsive to touch on the hand, particularly after nearly complete lesions ( $H = 27.843$ ,  $df = 17$ ,  $N = 240$ ,  $P = 0.047$ ); however, significant differences were not detected after the Bonferroni correction for multiple comparisons.

We observed unexpected single digit and small RFs in S2/PV in some cases. From our quantified data, we found greater response proportions with smaller RF sizes in S2/PV for intermediate-term cases that were exposed to the electrocutaneous stimulus versus tactile only ( $H = 17.33$ ,  $df = 7$ ,  $N = 39$ ,  $P = 0.015$ ). In area 1, we found the opposite tendency: greater response proportions with larger RF sizes ( $H = 21.172$ ,  $df = 7$ ,  $N = 50$ ,  $P = 0.004$ ). However, the pairwise comparisons were not significant after the Bonferroni correction. In area 3b, electrocutaneous stimulation exposure tended to result in greater proportions of GR with small RF sizes ( $H = 35.522$ ,  $df = 14$ ,  $N = 47$ ,  $P = 0.001$ ), but pairwise comparisons did not meet significance criteria.

Overall, the responses in S2/PV reflect the patterns in areas 3b and 1, with caveats. S2/PV did not reflect the same trends in response patterns associated with DCL conditions because S2/PV tended to respond better to stimulation on the hand in the more severe lesion conditions. Also, recovery time and lesion extent interacted to cause different effects, but the factor with greater influence over the responsive cortex was the lesion extent. The effects of complete DCL after long-term recovery resulted in greater proportions of large RFs in all areas, but S2/PV did not directly reflect area 3b in responsiveness and somatotopy related to DCL severity.

## Discussion

Our major findings in squirrel monkeys after DCL of varying extents and recovery times are the following. (1) Overall, neuronal responses in S2/PV typically reflected the patterns in area 1, which reflected the activation in area 3b. After less than 6 months of recovery from unilateral DCL that interrupted afferents from the hand, neurons in the hand regions in area 3b and higher-order somatosensory areas 1 and S2/PV were responsive to touch on the contralateral hand and forelimb. When the DCL was complete or nearly complete after longer recovery times (8–9 months), areas 3b, 1, and S2/PV underwent large-scale reorganization, in which responses to touch on face and forelimb could be found in the affected hand regions. (2) RFs of neurons in the deprived hand region in area 3b were usually larger with more extensive lesions, and similar trends were found in higher-order areas 1 and S2/PV. (3) Unexpectedly, neuronal responses to tactile stimulation at some recording sites in S2 and PV were stronger than those of areas 3b and 1.

Consistent with an earlier study using fMRI and microelectrode recordings in squirrel monkeys (Yang et al. 2014), the present results indicated that after months of recovery with incomplete DCL, neurons in the hand regions of areas 1 and S2/PV were responsive to touch on the contralateral hand and forelimb. The reactivation patterns were similar to those of area 3b, and most importantly, were similar to those of normal monkeys. However, with extensive DCL at high levels of the



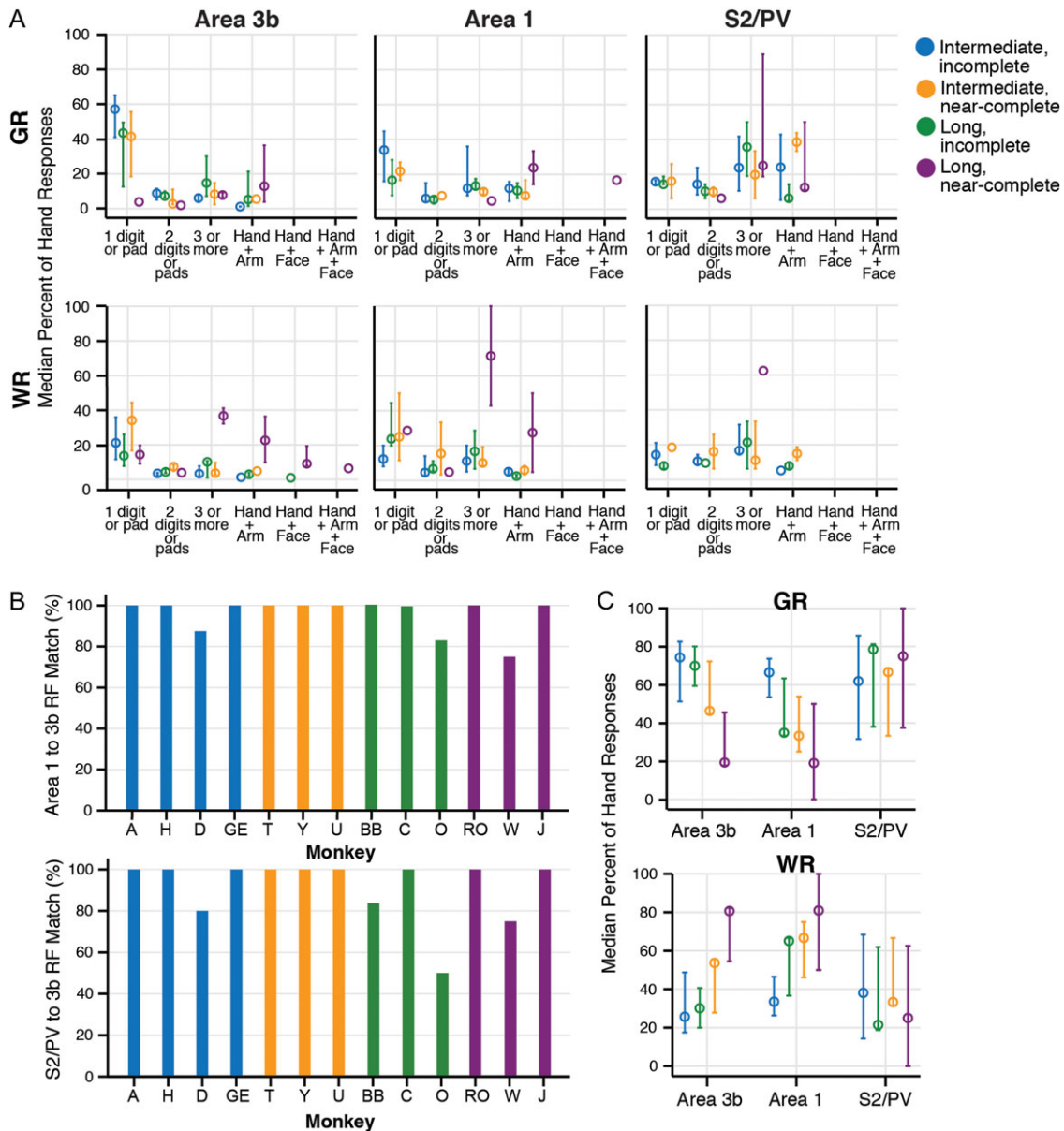


**Figure 7.** The percent of responses to the hand from areas of somatosensory cortex for all cases indicate that the effects of DCL on response strength and receptive field size vary by cortical area. Percent of weak responses (WR) and good responses (GR) were calculated from the total responses that included the hand for each monkey by area. Results are color-coded for the four categories of DCL and recovery times (open circles). A. Median percent of hand responses (y-axis) plotted in categories to represent size and type of response field (x-axis) show similarities between areas 3b, 1, and S2, particularly for weak responses. B. Percent of receptive field sites that were mapped in area 1 or S2/PV that were also mapped in area 3b, shown for each case. Receptive field (RF) sites were largely consistent between areas within each case, across DCL conditions. Receptive field (RF) sites mapped in area 1 corresponded to those mapped in area 3b (at 100%), with exception of three cases that matched between 75% and 87.5%. RF sites mapped in S2/PV were mapped in area 3b in most cases (at 100%), with four cases that matched between 50% and 83%. The presence of RF sites within location categories was counted to calculate the percent of matches:  $(RF_1 \text{ or } S2 \text{ matches to } RF_{3b}) / (\text{mapped } RF_1 \text{ or } S2 \text{ categories})$ . Response strength and the proportion of responses were not considered. RF location categories are similar to size categories in (A), but include individual digit representations for specificity within cases (see Supplementary Fig. S12). C. Receptive field sizes (from A) are summarized into the categories for each brain area to compare overall responsiveness in each area by DCL and recovery time. The median percent of GR in area 3b from cases with long-term (nearly) complete DCL tended to be reduced compared with other cases, but this was not reflected in S2/PV and area 1. The median percent of WR tends to increase after long-term complete DCL across cortical areas.

spinal cord after longer times of recovery (8–9 months), large-scale reorganizations usually occurred. Neurons in the affected hand regions in areas 3b, 1, and S2/PV became responsive to touch on the face and forelimb. The results of our comparisons between areas 3b and S2/PV after DCL in squirrel monkeys agree, in large part, with those of Tandon et al. (2009) in macaque monkeys with DCL. The large-scale reorganizations in somatosensory area 3b have been repeatedly reported in New

World and Old World monkeys after DCL (Jain et al. 1997, 1998, 2008) and in other sensory loss models. After a more extensive sensory loss produced by long-standing transections of the dorsal roots of the spinal cord that deprived the entire hand, forelimb, and shoulder, the entire hand-arm region of area 3b was activated by touch on face (Pons et al. 1991). Similarly, when Tandon et al. (2009) mapped areas 3b and S2/PV after long-term (>1 year) nearly complete DCLs in macaques, expansions of the

face representation into the expected hand territories were extensive in all cortical areas.

Interestingly, we did not find extensive expansions of face inputs into the affected hand region in areas 3b, 1, and S2/PV when the DCL were incomplete, or at slightly lower levels in the spinal cord so that inputs from the entire arm and shoulder survived the cuts. Since the main subdivision of the brainstem cuneate nucleus (rotunda) representing the hand of monkeys is encapsulated by the neurons representing the forelimb (Florence et al. 1989, 1991; Xu and Wall 1999), we suggest that these surviving inputs from the forelimb, along with those from the hand and digits prevent “face invasions” from the trigeminal system into the affected hand pathway. The post-lesion sprouting of these surviving inputs could activate deprived neurons in the cuneate nucleus, thereby preventing the reactivation by inputs from the face.

### Reactivation Patterns of Areas S2/PV Resemble those of Areas 3b and 1

One of the advantages of the present study is that we were able to perform quantitative analyses across different somatosensory areas within each monkey, and compare across monkeys with different conditions including the lesion extent and recovery time because of the relatively large sample size. Considering the neural responsiveness in areas 3b, 1, and S2/PV quantitatively, the lesion completeness tended to have more influence over responsiveness than the recovery time. Overall, we found that the lesion extent can exert different influences on different areas of somatosensory cortex. The proportion of responding neurons classified as weakly responsive to touch on hand in the deprived parts of areas 3b and 1 significantly increased with the lesion severity. In contrast, this effect of the lesion extent on neuronal responsiveness was less pronounced in areas S2/PV. Yet, comparisons of response patterns across areas 3b, 1, and S2/PV within the same monkeys revealed that the reactivation patterns in the primary and higher-order somatosensory cortex were strikingly similar despite the differences between monkeys in the lesion extent and recovery times.

In the cases with less extensive incomplete DCL, we found that hand regions in areas 3b, 1, and S2/PV were highly responsive, with more normal somatotopy and RF sizes. This favorable reactivation pattern was found particularly with shorter recovery times for areas 3b and 1, while in S2/PV the properties after longer recovery times tended to be as good as or better than those after intermediate recovery times. In the cases that had more severe lesions, long recovery times, and intensive behavioral training, larger-scale reorganizations were found in those areas. In monkeys with the nearly complete DCL and intermediate times of recovery, neurons in the deprived hand regions of areas 3b, 1, and S2/PV were not completely silent, but were less responsive to touch or taps on the hand compared with the monkeys with incomplete lesions. Another indication of the similarities between these somatosensory areas is that the presence of neurons with single digit RFs in areas S2/PV was usually concurrent with the presence of neurons with single digit RFs in area 3b. The similarities in the reactivation patterns between areas 3b, 1, and S2/PV in the present study support the functional importance of serial processing of somatosensory information in monkeys.

The issue of how tactile information is processed serially and in parallel from the thalamus to primary and higher-order somatosensory areas in primates is complicated, and remains a matter of debate (see Iwamura 1998; commentary “Revisiting

parallel and serial processing in the somatosensory system” from Garraghty in Dijkerman and de Haan 2007). Extensive connectivity studies demonstrated that higher-order somatosensory areas 1, S2, and PV receive strong, topographic inputs from area 3b (Friedman et al. 1980, 1986; Pons, Wall, et al. 1987; Pons et al. 1992; Burton and Fabri 1995; Krubitzer et al. 1995; Qi et al. 2002; Disbrow et al. 2003; Coq et al. 2004; Liao et al. 2013; Ashaber et al. 2014). Also, cortical lesion studies showed that ablations of the hand regions in somatosensory areas 3b, 1, and 2 of macaque monkeys initially eliminated tactile neuronal responses in S2 (Pons, Garraghty et al. 1987; Pons et al. 1988, 1992; Burton et al. 1990). Garraghty, Florence et al. also found that, “ablations of specific parts of the hand representations in areas 3a and 3b immediately deactivated the corresponding part of the hand representation in area 1” (1990), and ablations of areas 3a and 3b, immediately deactivated corresponding parts of PV (Garraghty, Pons, et al. 1990). However, Garraghty et al. (1991) also found that immediately after ablations of the forelimb region of the primary somatosensory area in prosimian primates and tree shrews, all parts of S2 remained highly responsive to cutaneous stimuli, suggesting a parallel processing of somatosensory information in these two species. Taken together, the anatomical and physiological findings support the hypothesis that the primary somatosensory cortex (S1), possibly area 3b, is the major driving source for cutaneous activation in area 1 and S2/PV in most anthropoid primates.

However, these higher-order areas not only receive direct inputs from the primary somatosensory cortex area 3b, but also from the thalamus, which could be an alternative source of cortical activation. Area 1, like area 3b, receives substantial thalamocortical inputs from neurons in the ventroposterior nucleus (VP) that primarily convey the tactile information (Jones and Powell 1970; Jones et al. 1979; Burton 1984), and these connections could independently activate area 1. S2, on the other hand, is innervated heavily by the inputs from the VPI and the posterior thalamus (Friedman and Murray 1986; Krubitzer and Kaas 1990, 1992; Qi et al. 2002), but sparsely from VP neurons that have comparable functional characteristics with those projecting to the area 3b (Krubitzer and Kaas 1992; Zhang et al. 2001; Qi et al. 2002; Wu and Kaas 2003). Since VPI and the posterior regions of the thalamus are parts of the spinothalamic system (e.g., Apkarian and Hodge 1989; Stevens et al. 1993; Stepniewska et al. 2003), these connections could send information about noxious stimuli, temperature, and touch to the S2 region (e.g., Craig 2006; Dum et al. 2009; for review see Craig 2002). Furthermore, Zhang and colleagues found that in marmosets, reversible inactivation of either S1 (Rowe et al. 1996) or S2 (Zhang et al. 1996) did not show strong impact on the magnitude of evoked potentials in the other area, similar to their findings in cats (Turman et al. 1992, 1995; Rowe et al. 1996). These results support a parallel network for tactile information in which S1 and S2 are hierarchically equivalent in most mammals studied, including at least some primate species.

Although results from the present study cannot directly explain how tactile information is processed in a serial or parallel fashion in squirrel monkeys, our observations that the reactivation patterns of area 1 and S2/PV resembled that of area 3b strongly suggested that the higher-order somatosensory areas likely depend on area 3b for cutaneous reactivation after DCL. However, we also found that some S2/PV hand neurons responded more strongly to tactile stimulation than those in area 3b. Previous studies have shown that areas S2/PV receive inputs from multiple cortical areas such as areas 3a,

3b, 1, 2, and motor cortex (Friedman et al. 1980; Friedman and Murray 1986; Cusick et al. 1989), and from several thalamic nuclei including the VPI nucleus, anterior pulvinar, and posterior nucleus of thalamus (Burton and Carlson 1986; Friedman and Murray 1986; Krubitzer and Kaas 1992; Qi et al. 2002), which are not directly affected by the DCL. Therefore, we speculate that the stronger responses observed in S2/PV are due to the convergence of subcortical and cortical projections to S2/PV that modulate the driving projections from areas 3b and 1. Alternatively, the convergence of several weak inputs from areas 3b and 1 on S2/PV neurons could produce stronger responses.

### Does Intensive Training Affect Cortical Reorganization after DCL?

Considerable evidence supports the overall conclusion that behavioral experience and activity-dependent plasticity are critical for restoring functions after losses including nerve cut (e.g., Florence et al. 2000), stroke (e.g., Nudo et al. 1996; Xerri et al. 1996; see Dobkin 2007 for review), dorsal rhizotomy (Darian-Smith and Ciferri 2005), and SCI (see Buonomano and Merzenich 1998; Jones 2000; Tetzlaff et al. 2009; Fouad and Tetzlaff 2012; Sofroniew 2018 for review). Our observations and quantitative analysis support the idea that hand use training promotes activity-dependent changes in behaviorally relevant ways (see Taub et al. 2006; Allred et al. 2014 for review).

For two cases matched by (nearly) complete DCL and long-term recovery (8–9 months), intensive training (SM-I) was associated with more responsiveness to touch or taps on the digits and hand in areas 3b and S2/PV than in the monkey without intervention (SM-W). In cases with incomplete DCL and intensive training, somatosensory areas underwent large-scale reorganization, such that spared inputs from the digits, hand, and forelimb expanded into deprived hand territories; and the responsiveness to touch or taps on hand and forelimb was much higher than that of monkeys without intensive training (regardless of recovery time). For instance, in monkey SM-Y, the representations of digits 1 and 2 were abnormally large in areas 3b and 1, and scattered digit 1 representations were present medially in the expected territories of deprived digits 4 and 5. We attribute this plasticity to the intense behavioral training that required coordination of all digits and palm, forelimb, hindlimb and trunk, although the reach-to-grasp task did not specifically reinforce the use of digit 1. Overall, these changes in neural reactivation in the deprived cortex were associated with behavioral recoveries of hand use in a reach-to-grasp task (Qi et al. 2013). However, if the lesion was complete and at a higher cervical level where the inputs from the entire hand and part of forelimb were below the lesion, training alone was not effective in restoring normal somatotopy and responsiveness. The persistent deficits in functional recovery are most likely due to a more complete loss of primary and secondary sensory inputs from the hand.

As training alone is not sufficient for full recoveries in patients after severe SCI, appropriate combinations of different types of interventions including biological and pharmacological treatments, and ES (all applied at optimized timings) may produce substantial improvement of anatomical and functional recovery (e.g., Courtine et al. 2009; Garcia-Alias et al. 2009; Schnell et al. 2011; Graziano et al. 2013; Weishaupt et al. 2013; Zhao and Fawcett 2013; see Rossignol et al. 2007; Kaas et al. 2008; Houle and Cote 2013; Reed et al. 2016 for review).

### Does electrocutaneous stimulation to the digits affect cortical reorganization after DCL?

Notable experimental and clinical studies indicate that sensorimotor ES plays a role in restoring function after spinal cord injury (SCI) and stroke. Since the 1960s, ES in the form of functional electrical stimulation (FES) has been used as a therapeutic application for patients with SCI to improve muscle activity to support and facilitate recoveries in standing, walking, hand grasping, and other body functions due to injuries (Barbeau et al. 2002; Donovan 2011; Rejc et al. 2017). FES uses safe levels of electrical current to activate the damaged or disabled neuromuscular system in a coordinated manner in order to restore lost functions. ES in the forms of somatosensory electrical stimulation (SES) has been also reported in patients with stroke. Wu et al. (2006) found that somatosensory stimulation applied to a paretic limb can improve performance of a functional test in patients with chronic stroke. This result supports the notion that SES in combination with training protocols may enhance the effects from neurorehabilitative treatments (see Kakulas 2004; Dobkin 2007; Hamid and Hayek 2008; Ragnarsson 2008; Edgerton and Harkema 2011; Veldman et al. 2014 for review). Although ES is widely used in clinical practice in patients with SCI and stroke, the mechanisms of how ES affects functional recovery at anatomical, physiological, and molecular levels are not fully understood. Our results provide preliminary insight that in monkeys that experienced ES, areas S2/PV tended to be more responsive to touch on the digits, have smaller RFs, and conformed more to normal somatotopic patterns. The effects of ES on the proportions of responsive and small RFs was supported by statistical analysis for areas S2/PV, but not for areas 3b and 1.

The underlying mechanisms of these observations remain unclear. The electrocutaneous stimulation activates not only the cutaneous afferents from digits via the dorsal columns and lateral funiculus in the spinal cord (Liao et al. 2015, 2018), but also pain and other sensations via the spinothalamic pathway (see Price and Mayer 1974; Kenshalo et al. 2000; Craig 2006; McGlone et al. 2014 for review). Because the spinothalamic pathway was not cut by the DCL, the ES may particularly strengthen this pathway, along with any other spared spinal cord afferents. The spinothalamic tract projects to several thalamic nuclei with different functional roles, including to the ventroposterior inferior (VPI) nucleus, and sparsely to the ventroposterior nucleus, both of which project to area 3b and other areas. However, the thalamic targets of the spinothalamic projections appear to terminate mainly in insular cortex, as well as areas S2 and PV and cingulate cortex, but only sparsely in areas 3b and 1 (Dum et al. 2009).

We conclude that after unilateral sensory loss due to DCL, both primary and higher-order somatosensory areas are partially or nearly fully reactivated over weeks to months of recovery. Across a wide range of lesion extents and recovery times, the reactivation patterns of higher-order somatosensory areas 1 and S2/PV closely reflect the reactivation patterns of area 3b, with some exceptions. The occasional stronger responses seen in deprived and recovered hand regions in S2 and PV may reflect convergence of inputs from other cortical areas, such as 3b and 1, along with parallel inputs from the VPI of the thalamus. In addition, task-related use of the impaired hand or electrocutaneous stimulation of the digits can promote recoveries of function and cortical properties in higher-order areas S2/PV, likely through the effects of activity-dependent plasticity on small numbers of surviving sensory inputs. Determining

whether painful levels of electrocutaneous stimulation are necessary to improve responsiveness in S2/PV, and whether such activation improves sensation, localization, and tactile object recognition are important considerations for use as a clinical intervention. Promising recoveries in subjects undergoing different types of ES combined with intensive task performance (rehabilitation) for spinal cord injury (e.g., Angeli et al. 2018; Inanici et al. 2018) indicate that mechanistic level knowledge is the next step forward for readily implemented treatment after injuries.

## Supplementary Material

Supplementary material is available at *Cerebral Cortex* online.

## Notes

The authors express our appreciation for generous contributions of Drs Christina M. Cerkevich, Limin Chen, Barbara C. Dillenburg, Robert Friedman, Mariana Gabi, Omar A. Gharbawie, Denis Matrov, Eva K. Sawyer, Barbara M.J. O'Brien, Emily C. Turner in data collection; Laura Trice provided expert technical assistance. This study was supported by NIH/NINDS grants NS067017 to H.-X.Q. and NS16446 to J.H.K., and a Craig H. Neilsen Foundation fellowship 314739 to J.L.R. and J.H.K. *Conflict of Interest*: None declared.

## References

- Allred RP, Kim SY, Jones TA. 2014. Use it and/or lose it—experience effects on brain remodeling across time after stroke. *Front Hum Neurosci*. 8:379.
- Andersen RA, Buneo CA. 2002. Intentional maps in posterior parietal cortex. *Annu Rev Neurosci*. 25:189–220.
- Angeli CA, Boakye M, Morton RA, Vogt J, Benton K, Chen Y, Ferreira CK, Harkema SJ. 2018. Recovery of over-ground walking after chronic motor complete spinal cord injury. *N Engl J Med*. 379:1244–1250.
- Apkarian AV, Hodge CJ. 1989. Primate spinothalamic pathways: I. A quantitative study of the cells of origin of the spinothalamic pathway. *J Comp Neurol*. 288:447–473.
- Ashaber M, Palfi E, Friedman RM, Palmer C, Jakli B, Chen LM, Kantor O, Roe AW, Negyessy L. 2014. Connectivity of somatosensory cortical area 1 forms an anatomical substrate for the emergence of multifinger receptive fields and complex feature selectivity in the squirrel monkey (*Saimiri sciureus*). *J Comp Neurol*. 522:1769–1785.
- Barbeau H, Ladouceur M, Mirbagheri MM, Kearney RE. 2002. The effect of locomotor training combined with functional electrical stimulation in chronic spinal cord injured subjects: walking and reflex studies. *Brain Res Brain Res Rev*. 40:274–291.
- Battaglia-Mayer A, Caminiti R. 2002. Optic ataxia as a result of the breakdown of the global tuning fields of parietal neurons. *Brain*. 125:225–237.
- Buonomano DV, Merzenich MM. 1998. Cortical plasticity: from synapses to maps. *Annu Rev Neurosci*. 21:149–186.
- Burton H. 1984. Corticothalamic connections from the second somatosensory area and neighboring regions in the lateral sulcus of macaque monkeys. *Brain Res*. 309:368–372.
- Burton H, Carlson M. 1986. Second somatic sensory cortical area (SII) in a prosimian primate, *Galago crassicaudatus*. *J Comp Neurol*. 247:200–220.
- Burton H, Fabri M. 1995. Ipsilateral intracortical connections of physiologically defined cutaneous representations in areas 3b and 1 of macaque monkeys: projections in the vicinity of the central sulcus. *J Comp Neurol*. 355:508–538.
- Burton H, Sathian K, Shao DH. 1990. Altered responses to cutaneous stimuli in the second somatosensory cortex following lesions of the postcentral gyrus in infant and juvenile macaques. *J Comp Neurol*. 291:395–414.
- Carlson M, Huerta MF, Cusick CG, Kaas JH. 1986. Studies on the evolution of multiple somatosensory representations in primates: the organization of anterior parietal cortex in the New World Callitrichid, *Saguinus*. *J Comp Neurol*. 246:409–426.
- Chen LM, Qi HX, Kaas JH. 2012. Dynamic reorganization of digit representations in somatosensory cortex of nonhuman primates after spinal cord injury. *J Neurosci*. 32:14649–14663.
- Coq JO, Qi H, Collins CE, Kaas JH. 2004. Anatomical and functional organization of somatosensory areas of the lateral fissure of the New World titi monkey (*Callicebus moloch*). *J Comp Neurol*. 476:363–387.
- Courtine G, Gerasimenko Y, van den Brand R, Yew A, Musienko P, Zhong H, Song B, Ao Y, Ichiyama RM, Lavrov I, et al. 2009. Transformation of nonfunctional spinal circuits into functional states after the loss of brain input. *Nat Neurosci*. 12:1333–1342.
- Craig AD. 2002. How do you feel? Interoception: the sense of the physiological condition of the body. *Nat Rev Neurosci*. 3:655–666.
- Craig AD. 2006. Retrograde analyses of spinothalamic projections in the macaque monkey: input to ventral posterior nuclei. *J Comp Neurol*. 499:965–978.
- Cusick CG, Wall JT, Felleman DJ, Kaas JH. 1989. Somatotopic organization of the lateral sulcus of owl monkeys: area 3b, S-II, and a ventral somatosensory area. *J Comp Neurol*. 282:169–190.
- Darian-Smith C, Brown S. 2000. Functional changes at periphery and cortex following dorsal root lesions in adult monkeys. *Nat Neurosci*. 3:476–481.
- Darian-Smith C, Ciferri M. 2006. Cuneate nucleus reorganization following cervical dorsal rhizotomy in the macaque monkey: its role in the recovery of manual dexterity. *J Comp Neurol*. 498:552–565.
- Darian-Smith C, Ciferri MM. 2005. Loss and recovery of voluntary hand movements in the macaque following a cervical dorsal rhizotomy. *J Comp Neurol*. 491:27–45.
- Dijkerman HC, de Haan EH. 2007. Somatosensory processes subserving perception and action. *Behav Brain Sci*. 30:189–201. discussion 201–139.
- Disbrow E, Litinas E, Recanzone GH, Padberg J, Krubitzer L. 2003. Cortical connections of the second somatosensory area and the parietal ventral area in macaque monkeys. *J Comp Neurol*. 462:382–399.
- Dobkin BH. 2007. Behavioral, temporal, and spatial targets for cellular transplants as adjuncts to rehabilitation for stroke. *Stroke*. 38:832–839.
- Donovan WH. 2011. Ethics, health care and spinal cord injury: research, practice and finance. *Spinal Cord*. 49:162–174.
- Dum RP, Levinthal DJ, Strick PL. 2009. The spinothalamic system targets motor and sensory areas in the cerebral cortex of monkeys. *J Neurosci*. 29:14223–14235.
- Edgerton VR, Harkema S. 2011. Epidural stimulation of the spinal cord in spinal cord injury: current status and future challenges. *Expert Rev Neurother*. 11:1351–1353.
- Florence SL, Hackett TA, Strata F. 2000. Thalamic and cortical contributions to neural plasticity after limb amputation. *J Neurophysiol*. 83:3154–3159.



- Florence SL, Wall JT, Kaas JH. 1989. Somatotopic organization of inputs from the hand to the spinal gray and cuneate nucleus of monkeys with observations on the cuneate nucleus of humans. *J Comp Neurol.* 286:48–70.
- Florence SL, Wall JT, Kaas JH. 1991. Central projections from the skin of the hand in squirrel monkeys. *J Comp Neurol.* 311:563–578.
- Fouad K, Tetzlaff W. 2012. Rehabilitative training and plasticity following spinal cord injury. *Exp Neurol.* 235:91–99.
- Friedman DP, Jones EG, Burton H. 1980. Representation pattern in the second somatic sensory area of the monkey cerebral cortex. *J Comp Neurol.* 192:21–41.
- Friedman DP, Murray EA. 1986. Thalamic connectivity of the second somatosensory area and neighboring somatosensory fields of the lateral sulcus of the macaque. *J Comp Neurol.* 252:348–373.
- Friedman DP, Murray EA, O'Neill JB, Mishkin M. 1986. Cortical connections of the somatosensory fields of the lateral sulcus of macaques: evidence for a corticolimbic pathway for touch. *J Comp Neurol.* 252:323–347.
- Gallyas F. 1979. Silver staining of myelin by means of physical development. *Neurol Res.* 1:203–209.
- Garcia-Alias G, Barkhuysen S, Buckle M, Fawcett JW. 2009. Chondroitinase ABC treatment opens a window of opportunity for task-specific rehabilitation. *Nat Neurosci.* 12:1145–1151.
- Garraghty PE, Florence SL, Kaas JH. 1990. Ablations of areas 3a and 3b of monkey somatosensory cortex abolish cutaneous responsivity in area 1. *Brain Res.* 528:165–169.
- Garraghty PE, Florence SL, Tenhula WN, Kaas JH. 1991. Parallel thalamic activation of the first and second somatosensory areas in prosimian primates and tree shrews. *J Comp Neurol.* 311:289–299.
- Garraghty PE, Kaas JH. 1991. Functional reorganization in adult monkey thalamus after peripheral nerve injury. *Neuroreport.* 2:747–750.
- Garraghty PE, Pons TP, Kaas JH. 1990. Ablations of areas 3b (SI proper) and 3a of somatosensory cortex in marmosets deactivate the second and parietal ventral somatosensory areas. *Somatosens Mot Res.* 7:125–135.
- Gharbawie OA, Stepniewska I, Kaas JH. 2011. Cortical connections of functional zones in posterior parietal cortex and frontal cortex motor regions in new world monkeys. *Cereb Cortex.* 21:1981–2002.
- Gibson AR, Hansma DI, Houk JC, Robinson FR. 1984. A sensitive low artifact TMB procedure for the demonstration of WGA-HRP in the CNS. *Brain Res.* 298:235–241.
- Graziano A, Foffani G, Knudsen EB, Shumsky J, Moxon KA. 2013. Passive exercise of the hind limbs after complete thoracic transection of the spinal cord promotes cortical reorganization. *PLoS One.* 8:e54350.
- Graziano A, Jones EG. 2009. Early withdrawal of axons from higher centers in response to peripheral somatosensory denervation. *J Neurosci.* 29:3738–3748.
- Hamid S, Hayek R. 2008. Role of electrical stimulation for rehabilitation and regeneration after spinal cord injury: an overview. *Eur Spine J.* 17:1256–1269.
- Houle JD, Cote MP. 2013. Axon regeneration and exercise-dependent plasticity after spinal cord injury. *Ann N Y Acad Sci.* 1279:154–163.
- Inanici F, Samejima S, Gad P, Edgerton VR, Hofstetter CP, Moritz CT. 2018. Transcutaneous electrical spinal stimulation promotes long-term recovery of upper extremity function in chronic Tetraplegia. *IEEE Trans Neural Syst Rehabil Eng.* 26:1272–1278.
- Iwamura Y. 1998. Hierarchical somatosensory processing. *Curr Opin Neurobiol.* 8:522–528.
- Jain N, Catania KC, Kaas JH. 1997. Deactivation and reactivation of somatosensory cortex after dorsal spinal cord injury. *Nature.* 386:495–498.
- Jain N, Catania KC, Kaas JH. 1998. A histologically visible representation of the fingers and palm in primate area 3b and its immutability following long-term deafferentations. *Cereb Cortex.* 8:227–236.
- Jain N, Florence SL, Qi HX, Kaas JH. 2000. Growth of new brainstem connections in adult monkeys with massive sensory loss. *Proc Natl Acad Sci USA.* 97:5546–5550.
- Jain N, Qi HX, Collins CE, Kaas JH. 2008. Large-scale reorganization in the somatosensory cortex and thalamus after sensory loss in macaque monkeys. *J Neurosci.* 28:11042–11060.
- Jones EG. 2000. Cortical and subcortical contributions to activity-dependent plasticity in primate somatosensory cortex. *Annu Rev Neurosci.* 23:1–37.
- Jones EG, Powell TP. 1970. Connexions of the somatic sensory cortex of the rhesus monkey. 3. Thalamic connexions. *Brain.* 93:37–56.
- Jones EG, Wise SP, Coulter JD. 1979. Differential thalamic relationships of sensory-motor and parietal cortical fields in monkeys. *J Comp Neurol.* 183:833–881.
- Kaas JH. 2004. Evolution of somatosensory and motor cortex in primates. *Anat Rec A Discov Mol Cell Evol Biol.* 281:1148–1156.
- Kaas JH, Florence SL. 1997. Mechanisms of reorganization in sensory systems of primates after peripheral nerve injury. *Adv Neurol.* 73:147–158.
- Kaas JH, Nelson RJ, Sur M, Lin CS, Merzenich MM. 1979. Multiple representations of the body within the primary somatosensory cortex of primates. *Science.* 204:521–523.
- Kaas JH, Qi HX, Burish MJ, Gharbawie OA, Onifer SM, Massey JM. 2008. Cortical and subcortical plasticity in the brains of humans, primates, and rats after damage to sensory afferents in the dorsal columns of the spinal cord. *Exp Neurol.* 209:407–416.
- Kakulas BA. 2004. Neuropathology: the foundation for new treatments in spinal cord injury. *Spinal Cord.* 42:549–563.
- Kambi N, Halder P, Rajan R, Arora V, Chand P, Arora M, Jain N. 2014. Large-scale reorganization of the somatosensory cortex following spinal cord injuries is due to brainstem plasticity. *Nat Commun.* 5:3602.
- Kenshalo DR, Iwata K, Sholas M, Thomas DA. 2000. Response properties and organization of nociceptive neurons in area 1 of monkey primary somatosensory cortex. *J Neurophysiol.* 84:719–729.
- Krubitzer L, Clarey J, Tweedale R, Elston G, Calford M. 1995. A redefinition of somatosensory areas in the lateral sulcus of macaque monkeys. *J Neurosci.* 15:3821–3839.
- Krubitzer LA, Kaas JH. 1990. The organization and connections of somatosensory cortex in marmosets. *J Neurosci.* 10:952–974.
- Krubitzer LA, Kaas JH. 1992. The somatosensory thalamus of monkeys: cortical connections and a redefinition of nuclei in marmosets. *J Comp Neurol.* 319:123–140.
- Liao CC, DiCarlo GE, Gharbawie OA, Qi HX, Kaas JH. 2015. Spinal cord neuron inputs to the cuneate nucleus that partially survive dorsal column lesions: a pathway that could contribute to recovery after spinal cord injury. *J Comp Neurol.* 523:2138–2160.

- Liao CC, Gharbawie OA, Qi H, Kaas JH. 2013. Cortical connections to single digit representations in area 3b of somatosensory cortex in squirrel monkeys and prosimian galagos. *J Comp Neurol.* 521:3768–3790.
- Liao CC, Reed JL, Kaas JH, Qi HX. 2016. Intracortical connections are altered after long-standing deprivation of dorsal column inputs in the hand region of area 3b in squirrel monkeys. *J Comp Neurol.* 524:1494–1526.
- Liao CC, Reed JL, Qi HX, Sawyer EK, Kaas JH. 2018. Second-order spinal cord pathway contributes to cortical responses after long recoveries from dorsal column injury in squirrel monkeys. *Proc Natl Acad Sci USA.* 115:4258–4263.
- McGlone F, Wessberg J, Olausson H. 2014. Discriminative and affective touch: sensing and feeling. *Neuron.* 82:737–755.
- Merzenich MM, Kaas JH, Sur M, Lin CS. 1978. Double representation of the body surface within cytoarchitectonic areas 3b and 1 in “SI” in the owl monkey (*Aotus trivirgatus*). *J Comp Neurol.* 181:41–73.
- Merzenich MM, Kaas JH, Wall J, Nelson RJ, Sur M, Felleman D. 1983. Topographic reorganization of somatosensory cortical areas 3b and 1 in adult monkeys following restricted deaf-ferentation. *Neuroscience.* 8:33–55.
- Merzenich MM, Kaas JH, Wall JT, Sur M, Nelson RJ, Felleman DJ. 1983. Progression of change following median nerve section in the cortical representation of the hand in areas 3b and 1 in adult owl and squirrel monkeys. *Neuroscience.* 10:639–665.
- Merzenich MM, Nelson RJ, Kaas JH, Stryker MP, Jenkins WM, Zook JM, Cynader MS, Schoppmann A. 1987. Variability in hand surface representations in areas 3b and 1 in adult owl and squirrel monkeys. *J Comp Neurol.* 258:281–296.
- Mowery TM, Kostylev PV, Garraghty PE. 2014. AMPA and GABA (A/B) receptor subunit expression in the cuneate nucleus of adult squirrel monkeys during peripheral nerve regeneration. *Neurosci Lett.* 559:141–146.
- Mowery TM, Sarin RM, Kostylev PV, Garraghty PE. 2015. Differences in AMPA and GABAA/B receptor subunit expression between the chronically reorganized cortex and brainstem of adult squirrel monkeys. *Brain Res.* 1611:44–55.
- Nudo RJ, Wise BM, SiFuentes F, Milliken GW. 1996. Neural substrates for the effects of rehabilitative training on motor recovery after ischemic infarct. *Science.* 272:1791–1794.
- Padberg J, Franca JG, Cooke DF, Soares JG, Rosa MG, Fiorani M Jr., Gattass R, Krubitzer L. 2007. Parallel evolution of cortical areas involved in skilled hand use. *J Neurosci.* 27:10106–10115.
- Pons TP, Garraghty PE, Friedman DP, Mishkin M. 1987. Physiological evidence for serial processing in somatosensory cortex. *Science.* 237:417–420.
- Pons TP, Garraghty PE, Mishkin M. 1988. Lesion-induced plasticity in the second somatosensory cortex of adult macaques. *Proc Natl Acad Sci USA.* 85:5279–5281.
- Pons TP, Garraghty PE, Mishkin M. 1992. Serial and parallel processing of tactual information in somatosensory cortex of rhesus monkeys. *J Neurophysiol.* 68:518–527.
- Pons TP, Garraghty PE, Ommaya AK, Kaas JH, Taub E, Mishkin M. 1991. Massive cortical reorganization after sensory deaf-ferentation in adult macaques. *Science.* 252:1857–1860.
- Pons TP, Kaas JH. 1986. Corticocortical connections of area 2 of somatosensory cortex in macaque monkeys: a correlative anatomical and electrophysiological study. *J Comp Neurol.* 248:313–335.
- Pons TP, Wall JT, Garraghty PE, Cusick CG, Kaas JH. 1987. Consistent features of the representation of the hand in area 3b of macaque monkeys. *Somatosens Res.* 4:309–331.
- Price DD, Mayer DJ. 1974. Physiological laminar organization of the dorsal horn of *M. mulatta*. *Brain Res.* 79:321–325.
- Qi HX, Chen LM, Kaas JH. 2011. Reorganization of somatosensory cortical areas 3b and 1 after unilateral section of dorsal columns of the spinal cord in squirrel monkeys. *J Neurosci.* 31:13662–13675.
- Qi HX, Gharbawie OA, Wong P, Kaas JH. 2011. Cell-poor septa separate representations of digits in the ventroposterior nucleus of the thalamus in monkeys and prosimian galagos. *J Comp Neurol.* 519:738–758.
- Qi HX, Gharbawie OA, Wynne KW, Kaas JH. 2013. Impairment and recovery of hand use after unilateral section of the dorsal columns of the spinal cord in squirrel monkeys. *Behav Brain Res.* 252:363–376.
- Qi HX, Lyon DC, Kaas JH. 2002. Cortical and thalamic connections of the parietal ventral somatosensory area in marmoset monkeys (*Callithrix jacchus*). *J Comp Neurol.* 443:168–182.
- Qi HX, Reed JL, Gharbawie OA, Burish MJ, Kaas JH. 2014. Cortical neuron response properties are related to lesion extent and behavioral recovery after sensory loss from spinal cord injury in monkeys. *J Neurosci.* 34:4345–4363.
- Qi HX, Wang F, Liao CC, Friedman RM, Tang C, Kaas JH, Avison MJ. 2016. Spatiotemporal trajectories of reactivation of somatosensory cortex by direct and secondary pathways after dorsal column lesions in squirrel monkeys. *Neuroimage.* 142:431–453.
- Ragnarsson KT. 2008. Functional electrical stimulation after spinal cord injury: current use, therapeutic effects and future directions. *Spinal Cord.* 46:255–274.
- Rasmusson D. 1996a. Changes in the organization of the ventroposterior lateral thalamic nucleus after digit removal in adult raccoon. *J Comp Neurol.* 364:92–103.
- Rasmusson DD. 1996b. Changes in the response properties of neurons in the ventroposterior lateral thalamic nucleus of the raccoon after peripheral deafferentation. *J Neurophysiol.* 75:2441–2450.
- Reed JL, Liao CC, Qi HX, Kaas JH. 2016. Plasticity and recovery after dorsal column spinal cord injury in nonhuman primates. *J Exp Neurosci.* 10:11–21.
- Rejc E, Angeli CA, Atkinson D, Harkema SJ. 2017. Motor recovery after activity-based training with spinal cord epidural stimulation in a chronic motor complete paraplegic. *Sci Rep.* 7:13476.
- Rossignol S, Schwab M, Schwartz M, Fehlings MG. 2007. Spinal cord injury: time to move? *J Neurosci.* 27:11782–11792.
- Rowe MJ, Turman AB, Murray GM, Zhang HQ. 1996. Parallel organization of somatosensory cortical areas I and II for tactile processing. *Clin Exp Pharmacol Physiol.* 23:931–938.
- Rowland JW, Hawryluk GW, Kwon B, Fehlings MG. 2008. Current status of acute spinal cord injury pathophysiology and emerging therapies: promise on the horizon. *Neurosurg Focus.* 25:E2.
- Schmid AC, Chien JH, Greenspan JD, Garonzik I, Weiss N, Ohara S, Lenz FA. 2016. Neuronal responses to tactile stimuli and tactile sensations evoked by microstimulation in the human thalamic principal somatic sensory nucleus (ventral caudal). *J Neurophysiol.* 115:2421–2433.
- Schnell L, Hunanyan AS, Bowers WJ, Horner PJ, Federoff HJ, Gulló M, Schwab ME, Mendell LM, Arvanian VL. 2011. Combined delivery of Nogo-A antibody, neurotrophin-3 and the NMDA-NR2d subunit establishes a functional ‘detour’ in the hemisectioned spinal cord. *Eur J Neurosci.* 34:1256–1267.
- Sofroniew MV. 2018. Dissecting spinal cord regeneration. *Nature.* 557:343–350.

- Stepniewska I, Cerkevich CM, Kaas JH. 2016. Cortical connections of the caudal portion of posterior parietal cortex in prosimian galagos. *Cereb Cortex*. 26:2753–2777.
- Stepniewska I, Fang PC, Kaas JH. 2005. Microstimulation reveals specialized subregions for different complex movements in posterior parietal cortex of prosimian galagos. *Proc Natl Acad Sci USA*. 102:4878–4883.
- Stepniewska I, Sakai ST, Qi HX, Kaas JH. 2003. Somatosensory input to the ventrolateral thalamic region in the macaque monkey: potential substrate for parkinsonian tremor. *J Comp Neurol*. 455:378–395.
- Stevens RT, London SM, Apkarian AV. 1993. Spinothalamicocortical projections to the secondary somatosensory cortex (SII) in squirrel monkey. *Brain Res*. 631:241–246.
- Sur M, Nelson RJ, Kaas JH. 1982. Representations of the body surface in cortical areas 3b and 1 of squirrel monkeys: comparisons with other primates. *J Comp Neurol*. 211:177–192.
- Tandon S, Kambi N, Lazar L, Mohammed H, Jain N. 2009. Large-scale expansion of the face representation in somatosensory areas of the lateral sulcus after spinal cord injuries in monkeys. *J Neurosci*. 29:12009–12019.
- Taub E, Uswatte G, Mark VW, Morris DM. 2006. The learned nonuse phenomenon: implications for rehabilitation. *Eura Medicophys*. 42:241–256.
- Tetzlaff W, Fouad K, Kwon B. 2009. Be careful what you train for. *Nat Neurosci*. 12:1077–1079.
- Turman AB, Ferrington DG, Ghosh S, Morley JW, Rowe MJ. 1992. Parallel processing of tactile information in the cerebral cortex of the cat: effect of reversible inactivation of SI on responsiveness of SII neurons. *J Neurophysiol*. 67:411–429.
- Turman AB, Morley JW, Zhang HQ, Rowe MJ. 1995. Parallel processing of tactile information in cat cerebral cortex: effect of reversible inactivation of SII on SI responses. *J Neurophysiol*. 73:1063–1075.
- Veldman MP, Maffiuletti NA, Hallett M, Zijdwind I, Hortobagyi T. 2014. Direct and crossed effects of somatosensory stimulation on neuronal excitability and motor performance in humans. *Neurosci Biobehav Rev*. 47:22–35.
- Wang Z, Qi HX, Kaas JH, Roe AW, Chen LM. 2013. Functional signature of recovering cortex: Dissociation of local field potentials and spiking activity in somatosensory cortices of spinal cord injured monkeys. *Exp Neurol*. 249:132–143.
- Weishaupt N, Vavrek R, Fouad K. 2013. Training following unilateral cervical spinal cord injury in rats affects the contralateral forelimb. *Neurosci Lett*. 539:77–81.
- Wong-Riley M. 1979. Changes in the visual system of monocularly sutured or enucleated cats demonstrable with cytochrome oxidase histochemistry. *Brain Res*. 171:11–28.
- Woods TM, Cusick CG, Pons TP, Taub E, Jones EG. 2000. Progressive transneuronal changes in the brainstem and thalamus after long-term dorsal rhizotomies in adult macaque monkeys. *J Neurosci*. 20:3884–3899.
- Wu CW, Kaas JH. 2003. Somatosensory cortex of prosimian Galagos: physiological recording, cytoarchitecture, and corticocortical connections of anterior parietal cortex and cortex of the lateral sulcus. *J Comp Neurol*. 457:263–292.
- Wu CW, Seo HJ, Cohen LG. 2006. Influence of electric somatosensory stimulation on paretic-hand function in chronic stroke. *Arch Phys Med Rehabil*. 87:351–357.
- Xerri C, Coq JO, Merzenich MM, Jenkins WM. 1996. Experience-induced plasticity of cutaneous maps in the primary somatosensory cortex of adult monkeys and rats. *J Physiol Paris*. 90:277–287.
- Xu J, Wall JT. 1999. Evidence for brainstem and supra-brainstem contributions to rapid cortical plasticity in adult monkeys. *J Neurosci*. 19:7578–7590.
- Yang PF, Qi HX, Kaas JH, Chen LM. 2014. Parallel functional reorganizations of somatosensory areas 3b and 1, and S2 following spinal cord injury in squirrel monkeys. *J Neurosci*. 34:9351–9363.
- Zhang HQ, Murray GM, Coleman GT, Turman AB, Zhang SP, Rowe MJ. 2001. Functional characteristics of the parallel SI- and SII-projecting neurons of the thalamic ventral posterior nucleus in the marmoset. *J Neurophysiol*. 85:1805–1822.
- Zhang HQ, Murray GM, Turman AB, Mackie PD, Coleman GT, Rowe MJ. 1996. Parallel processing in cerebral cortex of the marmoset monkey: effect of reversible SI inactivation on tactile responses in SII. *J Neurophysiol*. 76:3633–3655.
- Zhao RR, Fawcett JW. 2013. Combination treatment with chondroitinase ABC in spinal cord injury—breaking the barrier. *Neurosci Bull*. 29:477–483.